

DYNAMIC STABILITY OF COMPOSITE SHELLS SUBJECTED TO HYGROTHERMAL ENVIORNMENT

A THESIS SUBMITTED IN PARTIAL FULFILLMENT

OF THE REQUIREMENTS FOR THE DEGREE OF

MASTER OF TECHNOLOGY

IN

CIVIL ENGINEERING

(STRUCTURAL ENGINEERING)

By

ROSALIN SAHOO

Roll No-209CE2045



DEPARTMENT OF CIVIL ENGINEERING

NATIONAL INSTITUTE OF TECHNOLOGY ROURKELA

ROURKELA-769008, ORISSA, INDIA

MAY, 2011

**DYNAMIC STABILITY OF COMPOSITE SHELLS
SUBJECTED TO HYGROTHERMAL ENVIORNMENT**

A THESIS SUBMITTED IN PARTIAL FULFILLMENT

OF THE REQUIREMENTS FOR THE DEGREE OF

MASTER OF TECHNOLOGY

IN

CIVIL ENGINEERING

(STRUCTURAL ENGINEERING)

By

ROSALIN SAHOO

Roll No-209CE2045

UNDER THE GUIDANCE OF

Prof. S.K. SAHU



**DEPARTMENT OF CIVIL ENGINEERING
NATIONAL INSTITUTE OF TECHNOLOGY ROURKELA
ROURKELA-769008, ORISSA, INDIA**

MAY, 2011



NATIONAL INSTITUTE OF TECHNOLOGY
ROURKELA – 769008, ORISSA
INDIA

This is to certify that the thesis entitled, “**DYNAMIC STABILITY OF COMPOSITE SHELLS SUBJECTED TO HYGROTHERMAL ENVIRONMENT**” submitted by **Rosalin Sahoo** in partial fulfillment of the requirement for the award of **Master of Technology** degree in **Civil Engineering** with specialization in **Structural Engineering** at the National Institute of Technology, Rourkela is an authentic work carried out by her under my supervision and guidance. To the best of my knowledge, the matter embodied in the thesis has not been submitted to any other University/Institute for the award of any degree or diploma.

Date: 25.05.11

Place: Rourkela

Prof. S.K. Sahu

Dept. of Civil Engineering

National Institute of Technology

Rourkela-769008

ACKNOWLEDGEMENTS

I would like to express my sincere gratitude to my guide, **Dr. S.K. Sahu**, Professor, Department of Civil Engineering, National Institute of Technology, Rourkela for kindly providing me an opportunity to work under his supervision and guidance. His encouragement, advice, help, monitoring of the work, inputs and research support throughout my studies are embodied in this dissertation. His ability to teach, depth of knowledge and ability to achieve perfection will always be my inspiration.

My sincere thanks to Director of the institute and Head of the Civil Engineering Department **Prof. M. Panda**, National Institute of Technology Rourkela, for their advice and providing necessary facility for my work.

I am very thankful to all the faculty members and staffs of Civil engineering department who assisted me in my research, as well as in my post graduate studies. I would also like to thank Dr. A. Patel for her support.

I would like to give thanks to all my batch mates, who have directly or indirectly helped me in my project work and completion of this report.

I would like to thank my parents, younger brother and other family members for their unconditional support, love and affection. Their encouragement and never ending kindness made everything easier to achieve.

Date: 25.05.11
Place: Rourkela

Rosalin Sahoo
Roll No.-209CE2045
M.Tech (Structural Engineering)
NIT, Rourkela

CONTENTS

Chapter-1	INTRODUCTION	1-4
1.1	Introduction	1
1.2	Importance of the Present Structural Stability Studies	1
Chapter-2	REVIEW OF LITERATURE	5-12
2.1	Introduction	5
2.2	Review on plates	5
2.2.1	Static analysis of composite plates subjected to hygrothermal load	5
2.2.2	Vibration of Composite Plates Under Hygrothermal Conditions	7
2.2.3	Stability of Composite Plates Under Hygrothermal Conditions	8
2.3	Review on shells	9
2.3.1	Static analysis of composite Shells subjected to hygrothermal load	9
2.3.2	Vibration of Composite Plates Under Hygrothermal Conditions	9
2.3.3	Stability of Composite Plates Under Hygrothermal Conditions	10
2.4	Aim & scope of present studies	11
Chapter-3	MATHEMATICAL FORMULATION	13-26
3.1	The Basic Problem	13
3.2	Proposed Analysis	14
3.3	Assumptions of the Analysis	15
3.4	Finite Element formulation	
3.4.1	The shell element	15
3.4.2	Governing Equations	16
3.4.3	Dynamic stability studies	16
3.4.4	Constitutive Relation	17
3.4.5	Strain Displacement relations	20
3.5	Finite Element Formulation	21
3.5.1	Stiffness matrix	21
3.5.2	Geometric stiffness matrix $[K_{Ge}^r]$	22
3.5.3	Geometric stiffness matrix $[K_{Ge}^a]$	22

3.6	Solution Process	24
3.7	Computer program	25
Chapter-4	RESULTS AND DISCUSSIONS	27- 65
4.1	Introduction	27
4.2	Boundary Condition	27
4.3	Non-dimensionalisation of parameters	28
4.4	Vibration, buckling & dynamic stability of composite panels	28
	4.4.1 Convergence Study	28
	4.4.2 Comparison with previous Studies	31
	4.4.2.1 Vibration of composite plates and shells subjected to hygrothermal environment	31
	4.4.2.2.1 Buckling of composite plates and shells subjected to hygrothermal environment	34
4.5	Numerical Results	35
	4.5.2.2 Effects of Temperature on Frequencies of Vibration	36
	4.4.3.2 Effects of Moisture Concentration on Frequencies of Vibration	37
	4.5.2.3 Effects of temperature on Critical Load	37
	4.5.2.4 Effects of Moisture Concentration on Critical Load	38
4.6	Dynamic stability of composite plate	38
	4.6.2 Effect of static load factor on instability regions of uniformly loaded symmetric plate	39
	4.6.3 Effects of temperature on excitation frequency	40
	4.6.4 Effects of moisture on excitation frequency	42
	4.6.5 Effects of aspect ratio on excitation frequency	44
	4.6.6 Effects of ply orientation on excitation frequency	46
	4.6.7 Effects of temperature & moisture on instability region	47
	4.6.8 Effects of degree of orthotropy on excitation frequency	49
	4.6.9 Effect of side to thickness ratio on excitation frequency	50
	4.6.10 Effect of boundary condition on excitation frequency	51

4.7	Dynamic stability of composite shells	52
4.7.1	Effect of static load factor on instability regions of uniformly loaded symmetric plate	52
4.7.2	Effects of temperature on excitation frequency	53
4.7.3	Effects of moisture on excitation frequency	54
4.7.4	Effects of curvature on excitation frequency	55
4.7.5	Effects of aspect ratio on excitation frequency	56
4.7.6	Effects of degree of orthotropy on excitation frequency	58
4.7.7	Effects of thickness on excitation frequency	61
4.7.8	Effect of shallowness ratio on excitation frequency	62
4.7.9	Effect of ply orientation on excitation frequency	64
Chapter-6	CONCLUSIONS	66-67
	Future Scope of studies	67
	REFERENCES	68-74

ABSTRACT

Structural components subjected to in plane periodic loads may undergo instability due to certain combinations of natural frequency and in plane load parameters which is called parametric resonance. Composite structural components are often subjected to various environmental loads during their service life. The presence of temperature and moisture concentration may significantly reduce the stiffness and strength of the structures and may affect some design parameter such as vibration and stability characteristics of the structures. To avoid the typical problems caused by vibrations and stability, it is important to determine natural frequency, critical buckling load and excitation frequency of the composite laminated structures, under hygrothermal conditions. Therefore the vibration, buckling and dynamic stability behavior of laminated composite shells subjected to hygrothermal loadings are studied in the present investigation. A simple laminated model is developed for the vibration and stability analysis of laminated composite shells subjected to hygrothermal conditions. A computer program based on FEM in MATLAB environment is developed to perform all necessary computations. An eight-node isoparametric element is employed in the present analysis with five degrees of freedom per node. Element elastic stiffness matrices, mass matrices, geometric stiffness matrix due to mechanical and hygrothermal loads and load vectors are derived using the principle of minimum potential energy. They are evaluated using the Gauss quadrature numerical integration technique. Quantitative results are presented to show the effects of curvature, ply-orientation, degree of orthotropy, geometry and number of layers of laminate on vibration, buckling and dynamic stability of composite shells for different temperatures and moisture concentrations.

NOMENCLATURE

The principal symbols used in this thesis are presented for easy reference.

English

a, b	plate dimensions along x and y axes, respectively
C, C_0	elevated and reference moisture concentrations
e_x, e_y, e_{xy}	Non-mechanical strains due to moisture and temperature
E_1, E_2	Young's moduli of a lamina along and across the fibers, respectively
FEM	finite element method
G_{12}, G_{13}, G_{23}	Shear moduli of a lamina with respect to 1, 2 and 3 axes
K_x, K_y, K_{xy}	Curvatures of the plate
M_x, M_y, M_{xy}	Internal moment resultants per unit length
M_x^i, M_y^i, M_{xy}^i	Initial internal moment resultants per unit length
M_x^N, M_y^N, M_{xy}^N	Non-mechanical moment resultants per unit length due to moisture and temperature.
N_i	Shape function at a node i
N_x, N_y, N_{xy}	In-plane internal force resultants per unit length.
N_x^a, N_y^a, N_{xy}^a	Applied in-plane forces per unit length
N_x^i, N_y^i, N_{xy}^i	In-plane initial internal force resultants per unit length
N_x^N, N_y^N, N_{xy}^N	In-plane non-mechanical force resultants per unit length due to moisture and temperature.

N_{xcr}	Critical buckling load in x-direction
q	External transverse static load
Q_x, Q_y	Transverse shear resultants.
Q_x^i, Q_y^i	Initial transverse shear resultants
t	Thickness of plate
T, T_0	Elevated and reference temperatures
u, v	Displacements of the mid-plane along x and y axes, respectively
u_i, v_i, w_i	Displacements of node i along x, y and z axes, respectively
w	Displacement along z axis
x, y, z	System of co-ordinate axes
z_{k-1}, z_k	Bottom and top distance of lamina from mid-plane

Greek

α	Shear correction factor
α_1, α_2	Thermal coefficients along 1 and 2 axes of a lamina, respectively
β_1, β_2	Moisture coefficients along 1 and 2 axes of a lamina, respectively
$\epsilon_x, \epsilon_y, \gamma_{xy}$	In-plane strains of the mid-plane.
θ	Fiber orientation in a lamina
θ_x, θ_y	Rotations of the plate about x and y axes
ν_{12}, ν_{21}	Poisson's ratios

$\frac{\partial}{\partial x}, \frac{\partial}{\partial y}$	Partial derivatives with respect to x and y
ρ	Mass density
ξ, η	Local natural co-ordinates of an element
ξ_i, η_i	Local natural co-ordinates of the element at i^{th} node
ϕ_x, ϕ_y	Shear rotations in x-z and y-z planes, respectively
ω_n	Natural frequency
Ω	Excitation frequency
R_x, R_y, R_{xy}	radii of curvature of shell

Mathematical Operators

$[]^{-1}$	Inverse of the matrix
$[]^T$	Transpose of the matrix

LIST OF TABLES

Table 1: Non-dimensionalisation of parameters	28
Table 2: Convergence of non-dimensional free vibration frequencies for SSSS 4 layer plates for different ply orientations at 325K temperature	29
Table3: Convergence of non-dimensional free vibration frequencies for SSSS 4 layer plates for different ply orientations at 0.1%moisture concentration	29
Table4: Convergence of non-dimensional free vibration frequencies for CCCC 4 layer plates for different ply orientations at 325 K temperature	30
Table5: Convergence of non-dimensional critical load for SSSS 4 layer plates for different ply orientations at 325K temperature	30
Table 6: Convergence of non-dimensional critical load for SSSS 4 layer plates for different ply orientations at 0.1% moisture concentration	31
Table 7: Comparison of non-dimensional free vibration frequencies for S2 (0/90/90/0) spherical shell at normal temperature	32
Table 8: Comparison of non-dimensional free vibration frequencies for SSSS (0/90/90/0) plates at 325K temperature	33
Table 9: Comparison of non-dimensional free vibration frequencies for SSSS (0/90/90/0) plate at 0.1% moisture concentration	33
Table 10: Comparison of natural frequencies for S2 (0/90/90/0) shell at 1% moisture concentration	34

Table 11: Comparison of non-dimensional critical load for SSSS (0/90/90/0) plates at 325K temperature and 0.1% moisture concentration 35

Table 12: Comparison of Non-dimensional buckling loads of a square simply Supported symmetric cross-ply cylindrical laminated shell panels 35



LIST OF FIGURES

Fig.1: Doubly curved panel under in-plane loading	13
Fig.2: Arbitrarily oriented laminated plate	14
Fig.3: Geometry of an N-layered laminate	14
Fig.4: Eight-noded isoparametric element	21
Fig.5: Effect of temperature on non-dimensional frequency of (45/-45/45/-45) laminate	36
Fig.6: Effect of moisture on non-dimensional frequency of (45/-45/45/-45) laminate	37
Fig.7: Effect of temperature on non-dimensional critical load of angle-ply laminate	38
Fig.8: Effect of moisture on non-dimensional critical load of angle-ply laminate	38
Fig.9: Variations of instability region with static load factor of composite symmetric laminated plate subjected to hygrothermal loading	40
Fig.10: Variations of instability region with temperature of composite laminated symmetric cross-ply (0/90/90/0) plate	40
Fig.11: Variations of instability region with temperature of composite laminated anti-symmetric angle-ply (45/-45/45/-45) plate	41
Fig.12: Variations of instability region with temperature of composite laminated CCCC symmetric cross-ply (0/90/90/0) plate	42
Fig.13: Variations of instability region with moisture of composite laminated symmetric cross-ply (0/90/90/0) plate	42
Fig.14: Variations of instability region with moisture of composite laminated antisymmetric angle-ply (45/-45/45/-45) plate	43
Fig.15: Variations of instability region with moisture of composite laminated CCCC symmetric cross-ply (0/90/90/0) plate	43

Fig.16: Effect of aspect ratio on instability region of (45/-45/45/-45) laminate with elevated temperature	44
Fig.17: Effect of aspect ratio on instability region of CCCC anti symmetric angle-ply (45/-45/45/-45) laminate with elevated temperature	45
Fig.18: Effect of aspect ratio on instability region of CCCC anti symmetric angle-ply (45/-45/45/-45) laminate with elevated moisture	45
Fig.19: Effect of different ply orientation on instability region of anti-symmetric angle-ply laminate for elevated temperature	46
Fig.20: Effect of different ply orientation on instability region of anti-symmetric angle-ply laminate for elevated moisture	47
Fig.21: Effect of temperature & moisture on instability region of laminated SSSS anti-symmetric angle-ply (45/-45/45/-45) laminate	48
Fig.22: Effect of temperature & moisture on instability region of laminated CCCC anti-symmetric angle-ply (45 -45 45 -45) laminate	48
Fig.23: Effect of degrees of orthotropy on instability region of anti-symmetric angle-ply laminate for elevated temperature	49
Fig.24: Effect of degrees of orthotropy on instability region of anti-symmetric angle-ply laminate for elevated moisture	49
Fig.25: Effect of b/h ratio on instability region of (45/-45/45/-45) laminate for elevated temperature	50
Fig.26: Effect of b/h ratio on instability region of (45/-45/45/-45) laminate for elevated moisture	51
Fig.27: Effect of different boundary condition on instability region of anti-symmetric angle-ply laminate with elevated temperature	51
Fig.28: Variations of instability region with static load factor of composite symmetric laminated shell subjected to hygrothermal loading	52
Fig.29: Variations of instability region with temperature of composite laminated symmetric cross-ply (0/90/90/0) curved panel	53
Fig.30: Variations of instability region with temperature of composite laminated antisymmetric angle-ply (45/-45/45/-45) curved panel	54
Fig.31: Variations of instability region with moisture of composite laminated symmetric cross-ply (0/90/90/0) shell	55

Fig32: Variations of instability region with moisture of composite laminated anti-symmetric angle-ply (45/-45/45/-45) shell	55
Fig33: Variations of curvature of composite laminated symmetric cross-ply (0/90/90/0) curved panel with elevated temperature	56
Fig.34: Effect of aspect ratio on instability region of (0/90/90/0) laminate for elevated temperature	57
Fig.35: Effect of aspect ratio on instability region of (45/-45/45/-45) laminate for elevated temperature	57
Fig.36: Effect of aspect ratio on instability region of (0/90/90/0) laminate for elevated moisture	57
Fig.37: Effect of aspect ratio on instability region of (45/-45/45/-45) laminate for elevated moisture	58
Fig.38: Effect of degree of orthotropy on instability region of (0/90/90/0) laminate for elevated temperature	59
Fig.39: Effect of degree of orthotropy on instability region of (45/-45/45/-45) laminate for elevated temperature	59
Fig.40: Effect of degree of orthotropy on instability region of (0/90/90/0) laminate for elevated moisture	60
Fig.41: Effect of degree of orthotropy on instability region of (45/-45/45/-45) laminate for elevated moisture	60
Fig.42: Effect of thickness on instability region of (0/90/90/0) laminate for elevated temperature ($R_x = R_y = 3.125, 2.5, 1.875$)	61
Fig.43: Effect of thickness on instability region of (45/-45/45/-45) laminate for elevated temperature ($R_x = R_y = 3.125, 2.5, 1.875$)	61
Fig.44: Effect of thickness on instability region of (0/90/90/0) laminate for elevated moisture ($R_x = R_y = 3.125, 2.5, 1.875$)	62
Fig.45: Effect of thickness on instability region of (45/-45/45/-45) laminate for elevated moisture ($R_x = R_y = 3.125, 2.5, 1.875$)	62
Fig.46: Effect of R_y/b on instability region of (0/90/90/0) laminate for elevated temperature ($R_x = 1.5, 2.5, 5$)	63
Fig.47: Effect of R_y/b on instability region of (0/90/90/0) laminate for elevated moisture ($R_x = 1.5, 2.5, 5$)	63

Fig.48: Effect of R_y/b on instability region of (45/-45/45/-45) laminate for elevated temperature ($R_x = 1.5, 2.5, 5$)	63
Fig.49: Effect of R_y/b on instability region of (45/-45/45/-45) laminate for elevated moisture ($R_x = 1.5, 2.5, 5$)	64
Fig.50: Effect of different ply orientation on instability region of anti-symmetric angle-ply laminate for elevated temperature	65
Fig.51: Effect of different ply orientation on instability region of anti-symmetric angle-ply laminate for elevated moisture	65

INTRODUCTION

Composite materials are being increasingly used in aerospace, civil, naval and other high-performance engineering applications due to their light weight, high-specific strength and stiffness, excellent thermal characteristics, ease in fabrication and other significant attributes. Structures used in the above fields are more often exposed to high temperature as well as moisture. The varying environmental conditions due to moisture absorption and temperature seem to have an adverse effect on the stiffness and strength of the structural composites. This wide range of practical applications demands a fundamental understanding of their deformation, vibrations, static and dynamic stability characteristics in different temperature and moisture concentration.

1.1 Importance of the Present Structural Stability Studies

The aerospace organizations are intensively involved in the development of advanced composite materials for design, analysis and manufacturing of aircrafts and space vehicles. Composites are usually subjected to changing environmental conditions during both initial fabrication and final use. Among different environmental conditions that may influence composite mechanical behavior are the changes in temperature and moisture content. The effect of temperature is known as thermal effect and the effect of moisture absorption from the atmosphere is known as hygroscopic effect. The combined effects of temperature and moisture is known as hygrothermal effect. Heat gets conducted into the laminate when subjected to rise in the temperature. The laminate absorbs moisture when subjected to the wet conditions. The swelling or expansion is more across the fibres of the lamina. Hygrothermal effects induce a dimensional change in the lamina. But due to the mismatch of the properties of the constituents of the laminate, its free movement is inhibited. As a result, deformations and corresponding stress conditions are induced. The induced hygrothermal stresses is referred as residual stresses. The elastic properties and strength of the lamina, especially the matrix dominated one degrades. As a result the matrix-dominated properties such as stiffness and strength are altered. Hygrothermal expansions or contractions change the stress and strain distributions in the composite. So it is necessary to study and analyze the behavior such as buckling, natural frequencies and excitation frequencies of laminated composite shells under hygrothermal conditions.

Structural elements under in-plane periodic forces may undergo unstable transverse vibrations, leading to parametric resonance, due to certain combination of the values of in-plane load parameters and natural frequency of transverse vibration. This instability may occur below the critical load of the structure under compressive loads over a range or ranges of excitation frequencies. Several means of combating parametric resonance such as damping and vibration isolation may be inadequate and sometimes dangerous with reverse results. A number of catastrophic incidents can be traced to parametric resonance. In contrast to the principal resonance, the parametric instability may arise not merely at a single excitation frequency but even for small excitation amplitudes and combination of frequencies. Thus the parametric instability characteristics are of great technical importance for understanding the dynamic systems.

The distinction between ‘good’ and ‘bad’ vibration regimes of a structure, subjected to in-plane loading can be distinguished through a simple analysis of dynamic instability region (DIR) spectra. In its turn, the calculation of these spectra is often provided in terms of the spectrum of natural frequencies and the static buckling loads. Therefore it is an important task to calculate both of them with sufficiently high precision. Thus the study of dynamic stability itself requires a special investigation of basic problems of vibration and static stability.

Composites are vulnerable to environmental degradation. A moist environment, coupled with high or low temperature conditions is extremely detrimental for composites. There have been several efforts made by researchers in the last few years to establish the much needed correlation between the dynamical properties of the material and the moist environment or similar hygrothermal conditions.

As, the matrix is more susceptible to the hygrothermal condition than the fiber, the deformation is observed to be more in the transverse direction of the composite. The rise in moisture and temperature reduces the elastic moduli of the material and induces internal initial stresses, which may affect the stability as well as the safety of the structures. Hence, the changes in dynamic characteristics due to the hygrothermal effect seem to be an important consideration in composite analysis and design, which are of practical interest.

Composite materials are being increasingly used in automotive, marine and especially weight sensitive aerospace applications, primarily because of the large values of specific strength and these can be tailored through the variation of fibre orientation and stacking sequence to obtain an efficient design. The optimum design of laminated structures demands an effective analytical procedure. But the presence of various coupling stiffnesses and hygrothermal loading complicates the problem of dynamic stability analysis of composite structures in

addition to the inherent problem due to the boundary conditions encountered for obtaining a suitable theoretical solution. Even the real situation of boundaries in laminated structures is more complex because there are many types of boundary conditions that can be called simply-supported or clamped edges.

A comprehensive analysis of the dynamic stability problems on columns, rods, beams and pipes under various loads and boundary conditions has been studied exhaustively. The studies on dynamic stability of panels are scanty in literature. The dynamic stability of laminated composite panels, which has increasing applications in the aerospace structural components, is the subject of renewed interest by various researchers. Parametric resonance characteristics of plates and cylindrical shell structures are studied for uniform loading and certain boundary conditions. The dynamic stability of structures has been studied using first-order and higher-order shear deformation theories. A close perusal of the history of developments of dynamic stability class of problems indicates a renewed interest on the subject or various engineering especially, aerospace applications. In order to realize the full potential of these structures, a clear understanding of their stability behavior is a primary requirement.

The method of solution of dynamic stability class of problems involves first to reduce the equations of motion to a system of Mathieu-Hill equations having periodic coefficients and the parametric resonance characteristics are studied from the solution of the equations that are obtained from different methods of solution. In these analyses, the geometry of the structural components as well as its boundary conditions plays a major role in the choice of the methods of the solution. Analytical solutions are available only for certain geometry and boundary conditions. An attempt to have an analytical solution of the arbitrary geometry with non-classical boundary conditions may lead to an extremely tedious problem because of the complex nature of the solution. In a general structural problem, the governing Mathieu-Hill equations lead to an infinite set of equation with unknown coefficients which need to be truncated for finite degrees of freedom. The dynamic stability of plate and shell structures subjected to hygrothermal condition is studied by finite element methods.

The emergence of the digital computers with their enormous computing speed and core memory capacity has changed the outlook of the structural analysts and caused the evolution of various numerical methods such as the finite element, the finite strip method etc. For treating arbitrary loading and boundary conditions, the finite element is known to be one of the suitable methods because of its versatility. These numerical tools allow the researchers to model the structure in a more realistic manner with simpler mathematical forms.

It is clear from the above discussion, that the process of investigating the different aspects of dynamic stability of plates/shells structures with different temperature and moisture concentration is on, and hence, a study of dynamic stability behavior of structures with such an environment is a current problem of interest. The problem involves different complicated effect such as geometry, especially non-developable doubly curved surfaces, boundary conditions with variable temperature and moisture concentrations. The above discussed aspects need attention and thus constitute a problem of current interest.

A thorough review of earlier works done in this field is an important requirement to arrive at the objective and scope of the present investigation.

LITERATURE REVIEW

2.1 Introduction

The vast uses of conventional metals, its alloys and the ever increasing demand of composite materials in plates and shells are the subject of research for many years. Though the investigations is mainly focused on dynamic stability analysis of shell subjected to hygrothermal load, some relevant researches on vibration & buckling of plate & shell subjected to hygrothermal load and dynamic stability analysis of plates & shells are also studied for the sake of its relevance and completeness. Some of the pertinent studies done recently are reviewed elaborately and critically discussed to identify the lacunae in the existing literature. The studies in this are grouped into two major parts as follows:

- **Plates**
- **Shells**

In each section, the various aspects of analysis covered are

- Static analysis of composite panels subjected to hygrothermal load
- Vibration of composite panels subjected to hygrothermal load
- Stability of composite panels subjected to hygrothermal load

2.2 Reviews on Plates

The behavior of structures subjected to in-plane loads with hygrothermal load is less understood in comparison with structures under transverse loads. The following areas of analysis pertaining to the plates are covered in the review of literature:

2.2.1 Static analysis of composite plates subjected to hygrothermal load

The deformation and stress analysis of the laminated composite plates subjected to moisture and temperature has been the subject of research interest of many investigators. Ashton and Whitney (1971) studied the hygrothermal effects on bending, buckling and vibration of composite laminated plates using the Ritz method and neglecting the transverse shear deformation. Adams and Miller (1977) studied the effect of environment on the material properties of composite materials and observed that it has significant effect on strength and stiffness of the composites. Sairam and Sinha (1991) presented static analysis of laminated composites plates using First Order Shear Deformation Theory (FSDT) and employing finite element method. The effects of moisture and temperature on the deflections and stress

resultants are presented for simply supported and clamped anti-symmetric cross-ply and angle-ply laminates using reduced lamina properties at elevated moisture concentration and temperature. Lee *et al.* (1992) studied the influence of hygrothermal effects on the cylindrical bending of symmetric angle-ply laminated plates subjected to uniform transverse load for different boundary conditions via classical laminated plate theory and von-Karman's large deflection theory. The material properties of the composite are assumed to be independent of temperature and moisture variation. It has been observed that the classical laminated plate theory may not be adequate for the analysis of composite laminates even in the small deflection range. Shen (2002) studied the influence of hygrothermal effects on the nonlinear bending of shear deformable laminated plates using a micro-to-macro-mechanical analytical model and Reddy's higher order shear deformation plate theory. A perturbation technique is employed to determine the load-deflection and load-bending moment curves. Hygrothermal effects on the structural behavior of thick composite laminates using higher-order theory studied by Patel *et al.* (2002). Static and dynamic characteristics of thick composite laminates exposed to hygrothermal environment are studied using a realistic higher-order theory. The significance of retaining various higher-order terms in the present model, in evaluating the deflection, buckling and natural frequency for composite laminates at different moisture concentration and temperature. Rao and Sinha (2004) studied the effects of moisture and temperature on the bending characteristics of thick multidirectional fibrous composite plates. The finite element analysis accounts for the hygrothermal strains and reduced elastic properties of multidirectional composites at an elevated moisture concentration and temperature. Hygrothermal effect on dynamic interlaminar stresses in laminated plates with piezoelectric actuators studied by Wang *et al.* (2004). They studied the hygrothermal effect on the response histories and distribution of dynamic interlaminar stresses in laminated plates with piezoelectric actuator layers, under free vibration are studied, based on a hygrothermo-electrodynamic differential equations. Deflections and stresses are evaluated for thick multidirectional composite plates under uniform and linearly varying through-the-thickness moisture concentration and temperature. Results reveal the effects of fiber directionality on deflection and stresses. Hygrothermal effects on multilayered composite plates using a refined higher order theory studied by Lo *et al.* (2010). A four-node quadrilateral plate element based on the global-local higher order theory (GLHOT) is proposed to study the response of laminated composite plates due to a variation in temperature and moisture concentrations. Hygrothermal response due to a variation in temperature and moisture concentrations has been studied for different material types

sensitive to changing hygrothermal environment conditions. Upadhyay *et al.* (2010) studied the analytical solution of nonlinear flexural response of elastically supported cross-ply and angle-ply laminated composite plates under hygrothermal environment.

2.2.2 Vibration of composite plates subjected to hygrothermal load

The effect of environment on the free vibration of laminated plates has been considered earlier by Whitney and Ashton (1971). They used the Ritz method to analyze symmetric laminates and equilibrium equations of motion in the case of antisymmetric angle-ply laminates, based upon the classical laminated plate theory. A few results were presented for only symmetric angle-ply laminates. Dhanaraj and Palaninathan (1989) used the shell element to study the free vibrational characteristics of composite laminates under initial stress, which may also arise due to temperature. Results were presented showing how temperature affects the fundamental frequencies of anti-symmetric laminates. Sairam & Sinha (1992) focused their attention primarily on investigating the effects of moisture and temperature on the free vibration of laminated composite plates. The conventional finite element formulation is modified to include the strain energy of all types of initial stresses, viz. compressive, bending and shear stresses, developed due to moisture and temperature. The vibration characteristics of rectangular plates subjected to non-uniform loading are studied using power series method by Khukla *et al.* (1995) & differential quadrature method by Gutierrez *et al.* (1999). Lien-Wenchen, Chen (1988) studied vibrations of hygrothermal elastic composite plates. Nonlinear vibration & dynamic response of simply supported shear deformable laminated plates on elastic foundations studied by Huang, Zheng (2003). Nonlinear vibration & dynamic response of shear deformable laminated plates in hygrothermal condition studied by Zheng *et al.* (2004). Rao & Sinha (2004) studied dynamic response of multidirectional composites in hygrothermal environments. Jeyaraj *et al.* (2009) represented numerical studies on the vibration and acoustic response characteristics of a fiber-reinforced composite plate in a thermal environment by considering the inherent material damping property of the composite material. Initially the critical buckling temperature is obtained, followed by free and forced vibration analyses considering the pre-stress due to the imposed thermal environment. Panda & Singh (2009) presented nonlinear finite element model for geometrically large amplitude free vibration analysis of doubly curved composite spherical shell panel is presented using higher order shear deformation theory (HSDT).

2.2.3 Stability of composite plate subjected to hygrothermal load

The static stability or buckling of mechanical, civil engineering structures under compressive loading has always been an important field of research with the introduction of steel a century ago. The studies of temperature and moisture effects on the buckling loads of laminates are limited in number, and all these studies assumed perfectly initial configurations. Whitney and Ashton (1971) gave the first theoretical investigation of hygrothermal effects on the bending, buckling and vibration of composite laminated plates based on the classical laminated plate theory. The hygrothermal effects on the buckling of cylindrical composite panels were studied by Snead and Palazotto (1983) neglecting the transverse shear deformation effects, and by Lee and Yen (1989) including the transverse shear deformation effects. Ram and Sinha (1992) studied the hygrothermal effects on the buckling of composite laminated plates using the finite element method. Chao and Shyu (1996) calculated the buckling loads for composite laminated plates under hygrothermal environments, where a micro to- macro-mechanical analytical model was proposed. These analyses addressed initial buckling problems and were based on the first-order shear deformation plate theory (FSDPT). Shen (2002) studied the effect of hygrothermal conditions on the buckling and post buckling of shear deformable laminated cylindrical panels subjected to axial compression which is investigated using a micro-to-macro-mechanical analytical model. Eigen sensitivity analysis of moisture-related buckling of marine composite panels was studied by Barton (2007). He presented the elastic buckling of rectangular, symmetric angle-ply laminates subjected to a uniform moisture environment. This investigation presents an alternative method of computing the buckling load using Eigen values. Using this approach, an approximate closed-form expression is developed which can be used when exact solution are not available.

The studies on dynamic stability of structures are much less than in comparison to static stability & got a boost after Bolotin's (1964) contribution to the literature. The instability results of thin simply supported (1995) plates are sparsely treated in the literature. The instability of laminated composite plates considering geometric non-linearity is also reported using finite element method by Balamurugan *et al.* (1996). The instability of the elastic plates considering geometric non-linearity is also reported, through a finite element formulation by Ganapathi (2000). Partha & Singha (2006) studied the dynamic stability characteristics of simply supported laminated composite skew plates subjected to a periodic in-plane load are investigated using the finite element approach. The formulation includes the effects of transverse shear deformation, in-plane and rotary inertia. The boundaries of the instability

regions are obtained using the Bolotin's method and are represented in the non-dimensional load amplitude-excitation frequency plane. Liu (2007) started a mesh-free formulation for the static and free vibration analyses of composite plates is presented via a linearly conforming radial point interpolation method. The radial and polynomial basis functions are employed to construct the shape functions bearing Delta function property.

2.3 Reviews on Shells

The widespread use of shell structures in aerospace and hydrospace applications has stimulated many researchers to study various aspects of their structural behavior. In the present investigation an attempt has been made to the reviews on shells in the context of the present work and discussions are limited to the following areas of analysis

2.3.1 Static analysis of composite Shells subjected to hygrothermal load

The analyses of shells are more complicated due to the addition of curvature in the panel.

The finite element method is applied to study the problem of moisture and temperature effects on the stability of a general orthotropic cylindrical composite shell panel subjected to axial or in-plane shear loading by Lee & Yen (1989). The effect of hygrothermal conditions on the buckling and post buckling of shear deformable laminated cylindrical shells subjected to combined loading of axial compression and external pressure is investigated using micro-to-macro mechanical analytical model by Shen (2001). The hygrothermoelastic buckling behavior of laminated composite shells are numerically simulated using geometrically nonlinear finite element method was studied by Kundu & Han (2009). The effect of random system properties on the post buckling load of geometrically nonlinear laminated composite cylindrical shell panel subjected to hygrothermomechanical loading is investigated by Lal *et al.* (2010).

2.3.2 Vibration of composite Shells subjected to hygrothermal load

Huang and Tauchert (1991) investigated the large deformation behavior of anti-symmetric angle-ply laminates under non-uniform temperature loading. A finite element procedure for the geometrically nonlinear analysis of linear viscoelastic laminated composite systems subjected to mechanical and hygrothermal load was presented by Marques and Creus (1994). The formulation was implemented by considering three-dimensional degenerated shell element. The vibration response of flat and curved panels subjected to thermal and mechanical loads are presented by Librescu and Lin (1996). Gandhi *et al.* (1998) studied

nonlinear vibration of laminated composite plates in hygrothermal environments. In their analysis the formulations were based on the first-order shear deformable plate theory (FSDPT) and the numerical results were only for free vibration of a cantilevered laminated composite beam. Parhi *et al.*(2001) investigated the effect of moisture and temperature on the dynamic behavior of composite laminated plates and shells with or without delaminations. The dynamic analysis of laminated cross-ply composite non-circular thick cylindrical shells subjected to thermal/mechanical load is carried out based on higher-order theory was studied by Ganapathi *et al.* (2002). The nonlinear free vibration behavior of laminated composite shells subjected to hygrothermal environment was investigated by Naidu & Sinha (2006). The geometrically non-linear vibrations of linear elastic composite laminated shallow shells under the simultaneous action of thermal fields and mechanical excitations are analysed by Ribeiro & Jansen (2008). The vibration characteristics of pre- and post-buckled hygro-thermo-elastic laminated composite doubly curved shells was investigated by Kundu and Han(2009). Panda & Singh (2011) studied the nonlinear free vibration behaviour of single/dobly curved shell panel is addressed within the post-buckled state where thermal post-buckling of shell panel is accounted for a uniform temperature field.

2.3.3 Stability of composite Shells subjected to hygrothermal load

The parametric resonance characteristics of composite shells are studied by few investigators without considering the hygrothermal effects. The dynamic stability or phenomenon of parametric resonance in cylindrical shells under periodic loads has attracted much attention due to its detrimental and de-stabilizing effects in many engineering applications. This phenomenon in elastic systems was first studied by Bolotin (1964), where the dynamic instability regions were determined. Yao (1965) examined the non-linear elastic buckling and parametric excitation of a cylinder under axial loads. The parametric instability of circular cylindrical shells was also discussed by Vijayaraghavan and Evan-Iwanowskj (1967).

Based on the donnell's shell equations, the dynamic stability of circular cylindrical shells under both static and periodic compressive forces was examined by Nagai and Yamaki (1978) using Hsu's method. Bert and Birman (1990) extended Yao's (1965) approach to the parametric instability of thick orthotropic shells using higher-order theory. Liao and Cheng (1994) proposed a finite element model with a 3-D degenerated shell element and a 3-D degenerated curved beam element to investigate the dynamic stability of stiffened isotropic and laminated composites plates and shells subjected to in-plane periodic forces. Argento and Scott (1993) employed a perturbation technique to study the dynamic stability of layered

anisotropic circular cylindrical shells under axial loading. Using the same method, Argento (1993) later analyzed the dynamic stability of a composite circular cylindrical shell subjected to combined axial and torsional loading. The study of the parametric instability behavior of curved panels, the effects of curvature and aspect ratio on dynamic instability for a uniformly loaded laminated composite thick cylindrical panel is studied by Ganapathi *et al.* (1994) using finite element method. The dynamic stability of anti-symmetric cross-ply circular, cylindrical shells of different lamination schemes as well as the effect of the magnitude of the axial load on the instability regions was examined by NG *et al.* (1997). The dynamic instability of laminated composite circular cylindrical shells is studied by Ganapathi and Balamurugan (1998) using a C^0 shear flexible two noded axisymmetric shell element. The effects of various parameters such as ply angle, thickness, aspect ratio, axial and circumferential wave numbers on dynamic stability are studied. The dynamic stability of thin cross-ply laminated composite cylindrical shells under combined static and periodic axial force is investigated by NG *et al.* (1998) using Love's classical theory of thin shells. The effects of different lamination scheme and the magnitude of the axial load on the instability regions are examined using Bolotin's method. Most of the above mentioned investigators studied the dynamic stability of uniformly loaded closed cylindrical shells with a simply supported boundary condition. The parametric instability of laminated composite conical shells under periodic loads is studied of Ganapathi *et al.* (1999).

The dynamic stability behavior of laminated composite curved panels with cutouts subjected to in-plane static and periodic compressive loads was studied by Sahu & Dutta (2002). A numerical technique is developed for the dynamic stability analysis of composite laminated cylindrical shell under static and periodic axial forces by mesh-free kp-Ritz method by Liew *et al.* (2006). Quantitative results are presented to show the effects of curvature, ply-orientation, and degree of orthotropy, geometry and number of layers of laminate on dynamic stability of composite plates for different temperature and moisture concentrations.

2.4 Aim & scope of present studies

The present research is mainly aimed at filling up some of the lacunae that exists in the proper understanding of the dynamic stability of plates and shells. The application of in-plane loading and boundary conditions on the structural component will alter the global quantities such as frequency, buckling load and dynamic instability region (DIR). The problems are difficult in comparison to uniform in-plane stresses and may contain singularities during analysis.

The vast use of composite materials in every field of engineering compelled the author to have an extensive study on dynamic stability of composite plate/shell structures (curved panels) subjected to hygrothermal environment. In the present study, the parametric instability characteristics of plates/cylindrical/doubly curved composite panels subjected to hygrothermal loading are investigated using finite element method (FEM).

The influences of various parameters like effect of number of layers, static & dynamic load factors, side to thickness ratio, shallowness ratio, various boundary conditions, ply-orientations on the instability behavior of curved panels with different temperature and moisture concentrations have been examined. The present formulation of the problem is made general to accommodate a doubly curved panel with finite curvatures in both the directions with hygrothermal loading at different boundary conditions.

The different plate and shell problems identified for the present investigations are presented as follows.

Plates

- Effect of temperature and moisture on vibration of laminated composite plates.
- Effect of temperature and moisture on buckling of laminated composite plates.
- Effect of temperature and moisture on dynamic stability analysis of composite plates.

Shells

- Effect of temperature and moisture on vibration of laminated composite curved panels.
- Effect of temperature and moisture on buckling of laminated composite curved panels.
- Effect of temperature and moisture on dynamic stability analysis of composite curved panels.

MATHEMATICAL FORMULATION

3.1 The Basic Problems

The mathematical formulation for vibration, static and dynamic instability behavior of laminated composite plates and shells subjected to moisture and temperature are presented.

The basic configuration of the problem considered here is a doubly curved panel with in-plane loadings. The choice of the doubly curved panel geometry as a basic configuration has been made so that depending on the value of curvature parameter, plate, cylindrical panel and different doubly curved panels such as spherical configurations can be considered as special cases. The boundary conditions are incorporated in the most general manner to cater to the need of the curved boundary conditions.

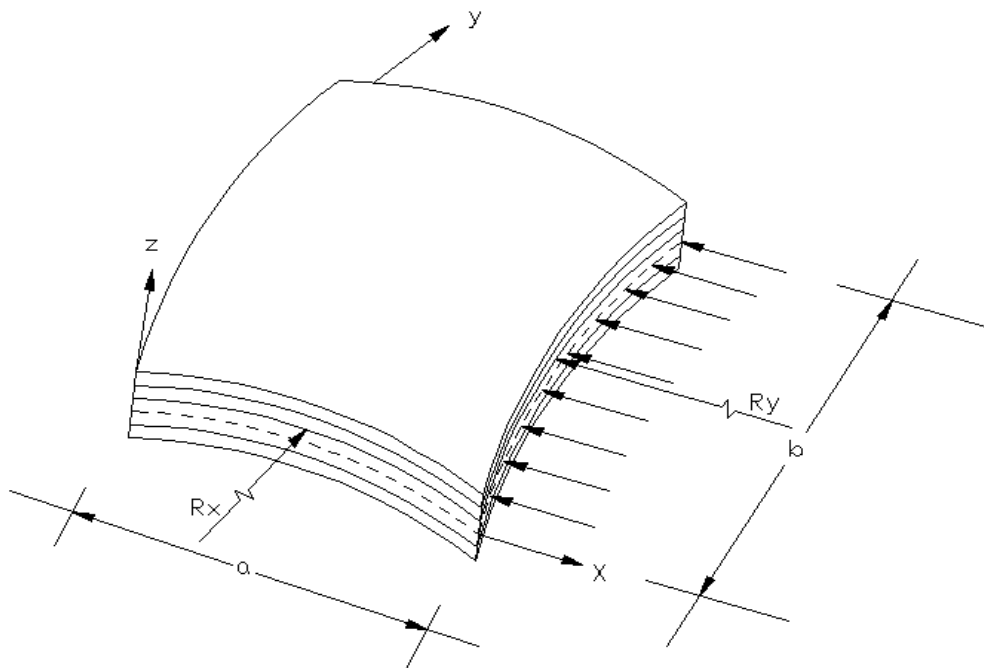


Fig.1 Doubly curved panel under in-plane loading

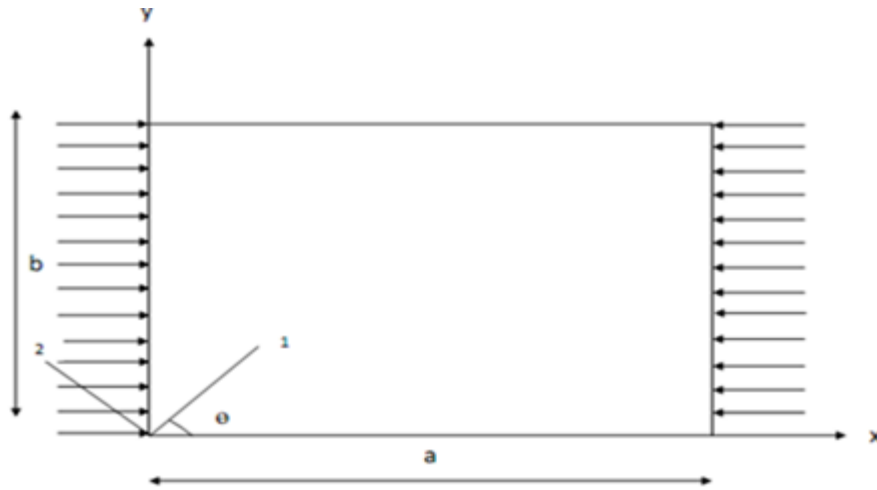


Fig.2 Arbitrary oriented laminated plate

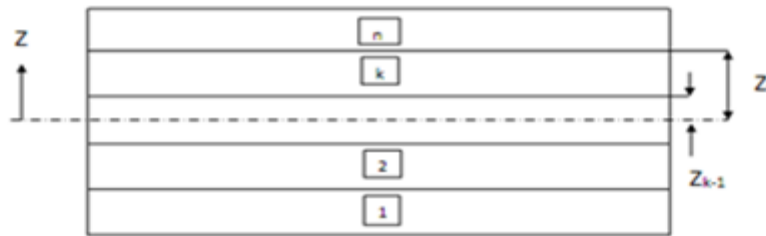


Fig.3 Geometry of an N-layered laminate

3.2 Proposed Analysis

The governing equations for the dynamic stability of laminated composite doubly curved panels/shells subjected to hygrothermal loading are developed. The presence of hygrothermal loading in the panel induces a non-uniform stress field in the structures. This necessitates the determination of stress field as a prerequisite to the solution of the problem like vibration, buckling and dynamic stability behavior of plates and shells with different temperature and moisture. As the thickness of the structure is relatively smaller, the determination of stress field reduces to the solution of a plane stress problem. The equation of motion represents a system of second order differential equation with periodic coefficients of the Mathieu-Hill type. The development of the regions of instability arises from Floquet's theory and the solution is obtained using Bolotin's approach using finite element method (FEM). The governing differential equations have been developed using first order shear deformation theory (FSDT). The assumptions made in this analysis are summarized as follows:

3.3 Assumptions of the Analysis

- 1) The analysis is linear with a few exceptions. This implies both linear constitutive relations (generalized Hooke's law for the material and linear kinematics) and small displacement to accommodate small deformation theory.
- 2) The curved panels are of various shapes with no initial imperfections. The considerations of imperfections are less important for dynamic loading.
- 3) This theory can be considered to be an extension of Sander's theory to doubly curved panels but generalized with tracers for different shell theories, considering transverse shear and rotary inertia. The straight line that is perpendicular to the neutral surface before deformation remains straight but not normal after deformation (FSDT). The thickness of the shell is small compared with the principal radii of curvature. Normal stress in z direction is neglected.
- 4) The loading considered is axial with a simple harmonic fluctuation with respect to time.
- 5) All damping effects are neglected.

3.4 Finite Element formulation

For problems involving complex in-plane loading and boundary conditions, analytical methods are not easily adaptable and numerical methods like finite element method (FEM) are preferred. Finite element formulation is developed hereby for the structural analysis of composite plate and shell structures with hygrothermal loading using a doubly curved shear deformable shell theory.

3.4.1 The shell element

An eight noded doubly curved isoparametric element is employed in the present analysis with five degrees of freedom u , v , w , θ_x and θ_y per node having all three radii of curvatures as shown in Fig.1. But the in-plane deformations u & v are considered for the initial plane stress analysis. The isoparametric element shall be oriented in the natural coordinate systems & shall be transferred to the Cartesian coordinate systems using the Jacobian matrix. In the analysis of thin shells where the element is assumed to have mid-surface nodes, the shape function of the element is derived using the interpolation polynomial. Consider a laminated panel of uniform thickness ' t ', consisting of a number of thin laminate, each of which may be arbitrarily oriented at an angle ' θ ' with reference to the X-axis of the co-ordinate system as shown in Figures 2 & 3.

3.4.2 Governing Equations

The governing differential equations for vibration of a shear deformable laminated composite plate in hygrothermal environment derived on the basis of first order shear deformation theory (FSDT) subjected to in-plane loads are:

$$\begin{aligned} \frac{\partial N_x}{\partial x} + \frac{\partial N_{xy}}{\partial y} - \frac{1}{2} \left(\frac{1}{R_y} - \frac{1}{R_x} \right) \frac{\partial M_{xy}}{\partial y} + \frac{Q_x}{R_x} + \frac{Q_y}{R_{xy}} &= P_1 \frac{\partial^2 u}{\partial t^2} + P_2 \frac{\partial^2 \theta_x}{\partial t^2} \\ \frac{\partial N_{xy}}{\partial x} + \frac{\partial N_y}{\partial y} + \frac{1}{2} \left(\frac{1}{R_y} - \frac{1}{R_x} \right) \frac{\partial M_{xy}}{\partial x} + \frac{Q_y}{R_y} + \frac{Q_x}{R_{xy}} &= P_1 \frac{\partial^2 v}{\partial t^2} + P_2 \frac{\partial^2 \theta_y}{\partial t^2} \\ \frac{\partial Q_x}{\partial x} + \frac{\partial Q_y}{\partial y} - \frac{N_x}{R_x} - \frac{N_y}{R_y} - 2 \frac{N_{xy}}{R_{xy}} + N_x^a \frac{\partial^2 w}{\partial x^2} + N_y^a \frac{\partial^2 w}{\partial y^2} + N_{xy}^a \frac{\partial^2 w}{\partial x \partial y} &= P_1 \frac{\partial^2 w}{\partial t^2} \\ \frac{\partial M_x}{\partial x} + \frac{\partial M_{xy}}{\partial y} - Q_x &= P_3 \frac{\partial^2 \theta_x}{\partial t^2} + P_2 \frac{\partial^2 u}{\partial t^2} \\ \frac{\partial M_{xy}}{\partial x} + \frac{\partial M_y}{\partial y} - Q_y &= P_3 \frac{\partial^2 \theta_y}{\partial t^2} + P_2 \frac{\partial^2 v}{\partial t^2} \end{aligned} \quad (1)$$

Where N_x , N_y and N_{xy} are the in-plane stress resultants, M_x , M_y and M_{xy} are moment resultants and Q_x , Q_y are transverse shear stress resultants. R_x , R_y and R_{xy} identify the radii of curvatures in the x and y direction and radius of twist.

$$(P_1, P_2, P_3) = \sum_{k=1}^n \int_{z_{k-1}}^{z_k} (\rho)_k (1, z, z^2) dz \quad (2)$$

Where n= number of layers of laminated composite curved panel, $(\rho)_k$ = mass density of k_{th} layer from mid-plane.

3.4.3 Dynamic stability studies

The equation of motion for vibration of a laminated composite panel in hygrothermal environment, subjected to generalized in-plane load $N(t)$ can be expressed in the matrix form as:

$$[M]\{\ddot{q}\} + [[K_e] - N(t)[K_g]]\{q\}=0 \quad (3)$$

‘q’ is the vector of degrees of freedoms (u, v, w, θ_x , θ_y). The in-plane load ‘N(t)’ may be harmonic and can be expressed in the form:

$$N(t) = N_s + N_t \cos \Omega t \quad (4)$$

Where N_s the static portion of load N (t), N_t the amplitude of the dynamic portion of N (t) and Ω is the frequency of the excitation. The stress distribution in the panel may be periodic considering the static and dynamic component of load as a function of the critical load,

$$N_s = \alpha N_{cr}, N_t = \beta N_{cr} \quad (5)$$

Where α and β are the static and dynamic load factors respectively. Using Eq. (5), the equation of motion for panel in hygrothermal environment under periodic loads in matrix form may be obtained as:

$$[M]\{\ddot{q}\} + [[K_e] - \alpha N_{cr}[K_g] - \beta N_{cr}[K_g] \cos \Omega t]\{q\} = 0 \quad (6)$$

The above Eq. (6) represents a system of differential equations with periodic coefficients of the Mathieu-Hill type. The development of regions of instability arises from Floquet's theory which establishes the existence of periodic solutions of periods T and 2T. The boundaries of the primary instability regions with period 2T, where $T = 2\frac{\pi}{\Omega}$ are of practical importance and the solution can be achieved in the form of the trigonometric series:

$$q(t) = \sum_{k=1,3,5}^{\infty} [\{a_k\} \sin(k\Omega t/2) + \{b_k\} \cos(k\Omega t/2)] \quad (7)$$

Putting this in Eq. (6) and if only first term of the series is considered, equating coefficients of $\sin \Omega t/2$ and $\cos \Omega t/2$, the equation (6) reduces to

$$[[K_e] - \alpha P_{cr}[K_g] \pm \frac{1}{2} \beta P_{cr}[K_g] - \frac{\Omega^2}{4}[M]]\{q\} = 0 \quad (8)$$

Eq.(8) represents an eigenvalue problem for known values of α, β and P_{cr} . The two conditions under the plus and minus sign correspond to two boundaries (upper and lower) of the dynamic instability region. The above eigenvalue solution give of Ω , which give the boundary frequencies of the instability regions for the given values of α and β . In this analysis, the computed static buckling load of the panel is considered as the reference load. Before solving the above equations, the stiffness matrix [K] is modified through imposition of boundary conditions.

3.4.4 Constitutive Relations

The constitutive relation for the plate, when subjected to moisture and temperature, are given by

$$\{F\} = [D] \{\varepsilon\} - \{F^N\} \dots \dots \dots (9)$$

Where

$$\begin{aligned} \{F\} &= \{N_x, N_y, N_{xy}, M_x, M_y, M_{xy}, Q_x, Q_y\}^T \\ \{F^N\} &= \{N_x^N, N_y^N, N_{xy}^N, M_x^N, M_y^N, M_{xy}^N, 0, 0\}^T \\ \{\varepsilon\} &= \{\varepsilon_x, \varepsilon_y, \gamma_{xy}, K_x, K_y, K_{xy}, \phi_x, \phi_y\}^T \end{aligned}$$

$$[D] = \begin{bmatrix} A_{11} & A_{12} & A_{16} & B_{11} & B_{12} & B_{16} & 0 & 0 \\ A_{12} & A_{22} & A_{26} & B_{12} & B_{22} & B_{26} & 0 & 0 \\ A_{16} & A_{26} & A_{66} & B_{16} & B_{26} & B_{66} & 0 & 0 \\ B_{11} & B_{12} & B_{16} & D_{11} & D_{12} & D_{16} & 0 & 0 \\ B_{12} & B_{22} & B_{26} & D_{12} & D_{22} & D_{26} & 0 & 0 \\ B_{16} & B_{26} & B_{66} & D_{16} & D_{26} & D_{66} & 0 & 0 \\ 0 & 0 & 0 & 0 & 0 & 0 & S_{44} & S_{45} \\ 0 & 0 & 0 & 0 & 0 & 0 & S_{45} & S_{55} \end{bmatrix}$$

Where,

N_x, N_y, N_{xy} = in-plane internal force resultants.

M_x, M_y, M_{xy} = internal moment resultants.

Q_x, Q_y = transverse shear resultants.

N_x^N, N_y^N, N_{xy}^N = in-plane non mechanical force resultants due to moisture and temperature.

M_x^N, M_y^N, M_{xy}^N = non-mechanical moment resultants due to moisture and temperature.

$\epsilon_x, \epsilon_y, \gamma_{xy}$ = in-plane strains of the mid-plane.

K_x, K_y, K_{xy} = curvature of the plate

Φ_x, ϕ_y = shear rotations in X-Z and Y-Z planes respectively.

A_{ij}, B_{ij}, D_{ij} and S_{ij} are the extensional, bending-stretching coupling, bending and transverse shear stiffnesses.

They may be defined as

$$A_{ij} = \sum_{k=1}^n (\bar{Q}_{ij})_k (Z_k - Z_{k-1})$$

$$B_{ij} = \frac{1}{2} \sum_{k=1}^n (\bar{Q}_{ij})_k (Z_k^2 - Z_{k-1}^2)$$

$$D_{ij} = \frac{1}{3} \sum_{k=1}^n (\bar{Q}_{ij})_k (Z_k^3 - Z_{k-1}^3) \quad \text{For } i, j = 1, 2, 6$$

$$S_{ij} = \alpha \sum_{k=1}^n (\bar{Q}_{ij})_k (Z_k - Z_{k-1}) \quad \text{For } i, j = 4, 5, \dots \dots \dots (10)$$

α = shear correction factor

Z_k, Z_{k-1} = bottom and top distance of lamina from mid-plane

The non-mechanical force and moment resultants are expressed as

$$\{ N_x^N, N_y^N, N_{xy}^N \}^T = \sum_{k=1}^n (\bar{Q}_{ij})_k \{ \epsilon \}_k (Z_k - Z_{k-1})$$

$$\{ M_x^N, M_y^N, M_{xy}^N \}^T = \frac{1}{2} \sum_{k=1}^n (\bar{Q}_{ij})_k \{ \epsilon \}_k (Z_k^2 - Z_{k-1}^2) \quad \text{For } i, j = 1, 2, 6, \dots \dots \dots (11)$$

Where $\{ \epsilon \}_k = \{ \epsilon_{xN}, \epsilon_{yN}, \epsilon_{xyN} \}^T = [T] \{ \beta_1, \beta_2 \}_k^T (C - C_0) + [T] \{ \alpha_1, \alpha_2 \}_k^T (T - T_0)$, in which

$$[T] = \begin{bmatrix} \cos^2 \theta & \sin^2 \theta \\ \sin^2 \theta & \cos^2 \theta \\ \sin 2\theta & -\sin 2\theta \end{bmatrix}$$

$\epsilon_{xN}, \epsilon_{yN}, \epsilon_{xyN}$ = non-mechanical strains due to moisture and temperature

β_1, β_2 = moisture coefficients along 1 and 2 axes of a lamina, respectively

α_1, α_2 = thermal coefficients along 1 and 2 axes of a lamina, respectively

T, T_0 = elevated and reference temperatures

C, C_0 = elevated and reference moisture concentrations

$\overline{(Q_{ij})}_k$ in equations (2) and (3) is defined as $\overline{(Q_{ij})}_k = [T_1]^T [Q_{ij}]_k [T_1]$

$$\overline{(Q_{ij})}_k = [T_1]^T [Q_{ij}]_k [T_1] \quad \text{For } i, j = 1, 2, 6$$

$$\overline{(Q_{ij})}_k = [T_2]^T [Q_{ij}]_k [T_2] \quad \text{For } i, j = 4, 5 \dots \dots \dots (12)$$

Where

$$[T_1] = \begin{bmatrix} \cos^2 \theta & \sin^2 \theta & 2 \sin \theta \cos \theta \\ \sin^2 \theta & \cos^2 \theta & -2 \sin \theta \cos \theta \\ -\sin \theta \cos \theta & \sin \theta \cos \theta & \cos^2 \theta - \sin^2 \theta \end{bmatrix}$$

$$[T_2] = \begin{bmatrix} \cos \theta & -\sin \theta \\ \sin \theta & \cos \theta \end{bmatrix}$$

$$[Q_{ij}]_k = \begin{bmatrix} Q_{11} & Q_{12} & 0 \\ Q_{21} & Q_{22} & 0 \\ 0 & 0 & Q_{66} \end{bmatrix} \quad \text{For } i, j = 1, 2, 6$$

$$[Q_{ij}]_k = \begin{bmatrix} Q_{44} & 0 \\ 0 & Q_{55} \end{bmatrix} \quad \text{For } i, j = 4, 5$$

In which

$$Q_{11} = E_1 / (1 - \nu_{12}\nu_{21})$$

$$Q_{12} = \nu_{12} E_2 / (1 - \nu_{12}\nu_{21})$$

$$Q_{22} = E_2 / (1 - \nu_{12}\nu_{21})$$

$$Q_{44} = G_{13}, Q_{55} = G_{23}$$

E_1, E_2 = Young's moduli of a lamina along and across the fibers, respectively

G_{12}, G_{13}, G_{23} = Shear moduli of a lamina with respect to 1, 2 and 3 axes.

Ψ_{12}, Ψ_{21} = Poisson's ratios

3.4.5 Strain Displacement relations

Green-Lagrange's strain displacement relations are presented in general throughout the analysis. The linear part of the strain is used to derive the elastic stiffness matrix and the non-

linear part of the strain is used to derive the elastic stiffness matrix and the non-linear part of the strain is used to derive the geometric stiffness matrix. The total strain is given by

$$\{\varepsilon\} = \{\varepsilon_l\} + \{\varepsilon_{nl}\} \quad (13)$$

The linear shear deformable Sanders' strain displacement relations are

$$\begin{aligned} \varepsilon_x &= \frac{\partial u}{\partial x} + \frac{w}{R_x} + zk_x \\ \varepsilon_y &= \frac{\partial v}{\partial y} + \frac{w}{R_y} + zk_y \\ \gamma_{xy} &= \frac{\partial u}{\partial y} + \frac{\partial v}{\partial x} + \frac{2w}{R_{xy}} + zk_{xy} \\ \gamma_{xz} &= \frac{\partial w}{\partial x} + \theta_x - \frac{u}{R_x} - \frac{v}{R_{xy}} \\ \gamma_{yz} &= \frac{\partial w}{\partial y} + \theta_y - \frac{v}{R_y} - \frac{u}{R_{xy}} \end{aligned} \quad (14)$$

The bending strains k_j are expressed as,

$$\begin{aligned} \kappa_x &= \frac{\partial \theta_x}{\partial x} & \kappa_y &= \frac{\partial \theta_y}{\partial y} \\ \kappa_{xy} &= \frac{\partial \theta_x}{\partial y} + \frac{\partial \theta_y}{\partial x} + \frac{1}{2} \left(\frac{1}{R_y} - \frac{1}{R_x} \right) \left(\frac{\partial v}{\partial x} - \frac{\partial u}{\partial y} \right) \end{aligned} \quad (15)$$

The nonlinear strain components are defined as follows:

$$\begin{aligned} \varepsilon_{xnl} &= \frac{1}{2} \left(\frac{\partial u}{\partial x} \right)^2 + \frac{1}{2} \left(\frac{\partial v}{\partial x} \right)^2 + \frac{1}{2} \left(\frac{\partial w}{\partial x} - \frac{u}{R_x} \right)^2 + \frac{1}{2} z^2 \left[\left(\frac{\partial \theta_x}{\partial x} \right)^2 + \left(\frac{\partial \theta_y}{\partial x} \right)^2 \right] \\ \varepsilon_{ynl} &= \frac{1}{2} \left(\frac{\partial u}{\partial y} \right)^2 + \frac{1}{2} \left(\frac{\partial v}{\partial y} \right)^2 + \frac{1}{2} \left(\frac{\partial w}{\partial y} - \frac{v}{R_y} \right)^2 + \frac{1}{2} z^2 \left[\left(\frac{\partial \theta_x}{\partial y} \right)^2 + \left(\frac{\partial \theta_y}{\partial y} \right)^2 \right] \\ \gamma_{xynl} &= \left(\frac{\partial u}{\partial x} \right) \left(\frac{\partial u}{\partial y} \right) + \left(\frac{\partial v}{\partial x} \right) \left(\frac{\partial v}{\partial y} \right) + \left(\frac{\partial w}{\partial x} - \frac{u}{R_x} \right) \left(\frac{\partial w}{\partial y} - \frac{v}{R_y} \right) + z^2 \left[\left(\frac{\partial \theta_x}{\partial x} \right) \left(\frac{\partial \theta_x}{\partial y} \right) + \left(\frac{\partial \theta_y}{\partial x} \right) \left(\frac{\partial \theta_y}{\partial y} \right) \right] \end{aligned} \quad (16)$$

u, v = displacements of the mid-plane along x and y axes, respectively

w = displacement along z axis

θ_x, θ_y = rotations of the plate about x and y axes.

3.5 Finite Element Formulation

For problems involving complex in-plane loading and boundary conditions numerical methods like finite element method (FEM) are preferred. Eight-nodded isoperimetric element is used to the present free vibration problem. Five degrees of freedom u, v, w, θ_x and θ_y are considered at each node. The stiffness matrix, the geometric stiffness matrix due to residual

stresses, geometric stiffness matrix due to applied in-plane loads and nodal load vector of the element are derived using the principle of minimum potential energy.

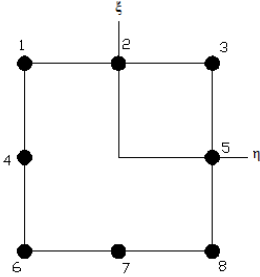


Fig.4 Eight noded isoparametric element

The element displacements are expressed in terms of their nodal values by using the element shape functions and are given by

$$\begin{aligned}
 u &= \sum_{i=1}^8 N_i u_i & v &= \sum_{i=1}^8 N_i v_i & w &= \sum_{i=1}^8 N_i w_i \\
 \theta_x &= \sum_{i=1}^8 N_i \theta_{xi} & \theta_y &= \sum_{i=1}^8 N_i \theta_{yi} \dots \dots \dots (17)
 \end{aligned}$$

N_i = Shape function at a node i

ξ, η = Local natural co-ordinates of an element

3.5.1 Stiffness matrix

The linear strain matrix $\{\epsilon\}$ is obtained by substituting equations (17) into (15), and is expressed as

$$\{\epsilon\} = [B] \{\delta_e\} \dots \dots \dots (18)$$

Where

$$\{\delta_e\} = \{u_1, v_1, w_1, \theta_{x1}, \theta_{y1}, \dots \dots \dots, u_8, v_8, w_8, \theta_{x8}, \theta_{y8}\}^T$$

$$[B] = \begin{bmatrix} \frac{\partial N_i}{\partial x} & 0 & \frac{N_i}{R_x} & 0 & 0 \\ 0 & \frac{\partial N_i}{\partial x} & \frac{N_i}{R_y} & 0 & 0 \\ \frac{\partial N_i}{\partial y} & \frac{\partial N_i}{\partial x} & 0 & 0 & 0 \\ 0 & 0 & 0 & 0 & \frac{\partial N_i}{\partial x} \\ 0 & 0 & 0 & \frac{\partial N_i}{\partial y} & 0 \\ 0 & 0 & 0 & \frac{\partial N_i}{\partial x} & \frac{\partial N_i}{\partial y} \\ 0 & 0 & \frac{\partial N_i}{\partial x} & 0 & N_i \\ 0 & 0 & \frac{\partial N_i}{\partial y} & N_i & 0 \end{bmatrix} \quad \text{For } i= 1, 2, \dots \dots \dots 8$$

The element stiffness matrix is given by

$$[K_e] = \iint [B]^T [D] [B] dx dy \dots \dots \dots (19)$$

3.5.2 Geometric stiffness matrix $[K_{Ge}^r]$

The non-linear strains, equations (6), are represented in matrix form as

$$\{\varepsilon_{nl}\} = \{\varepsilon_{xnl}, \varepsilon_{ynl}, \gamma_{xynl}, \gamma_{xznl}, \gamma_{yznl}\}^T = [R] \{d\} / 2, \dots \dots \dots (20)$$

Where $\{d\} = \left\{ \left(\frac{\partial u}{\partial x}\right), \left(\frac{\partial u}{\partial y}\right), \left(\frac{\partial v}{\partial x}\right), \left(\frac{\partial v}{\partial y}\right), \left(\frac{\partial w}{\partial x}\right), \left(\frac{\partial w}{\partial y}\right), \left(\frac{\partial \theta_x}{\partial x}\right), \left(\frac{\partial \theta_x}{\partial y}\right), \left(\frac{\partial \theta_y}{\partial x}\right), \left(\frac{\partial \theta_y}{\partial y}\right), \theta_x, \theta_y \right\}^T$

By using equations (17), $\{d\}$ may be expressed as

$$\{d\} = [G] \{\delta_e\} \dots \dots \dots (21)$$

Where

$$[G] = \begin{bmatrix} \frac{\partial N_i}{\partial x} & 0 & 0 & 0 & 0 \\ \frac{\partial N_i}{\partial y} & 0 & 0 & 0 & 0 \\ 0 & \frac{\partial N_i}{\partial x} & 0 & 0 & 0 \\ 0 & \frac{\partial N_i}{\partial y} & 0 & 0 & 0 \\ -\frac{N_i}{R_x} & 0 & \frac{\partial N_i}{\partial x} & 0 & 0 \\ 0 & -\frac{N_i}{R_y} & \frac{\partial N_i}{\partial y} & 0 & 0 \\ 0 & 0 & 0 & \frac{\partial N_i}{\partial x} & 0 \\ 0 & 0 & 0 & \frac{\partial N_i}{\partial y} & 0 \\ 0 & 0 & 0 & 0 & \frac{\partial N_i}{\partial x} \\ 0 & 0 & 0 & 0 & \frac{\partial N_i}{\partial y} \\ 0 & 0 & 0 & 1 & 0 \\ 0 & 0 & 0 & 0 & 1 \end{bmatrix} \text{ For } i = 1, 2, \dots, 8$$

The initial stress stiffness matrix is given by

$$[K_{Ge}^r] = \iint [G]^T [S] [G] dx dy \dots \dots \dots (22)$$

Where

$$[N] = \begin{bmatrix} Ni & 0 & 0 & 0 & 0 \\ 0 & Ni & 0 & 0 & 0 \\ 0 & 0 & Ni & 0 & 0 \\ 0 & 0 & 0 & Ni & 0 \\ 0 & 0 & 0 & 0 & Ni \end{bmatrix} \quad \text{For } i = 1, 2, \dots, 8$$

$$[P] = \begin{bmatrix} P_1 & 0 & 0 & P_2 & 0 \\ 0 & P_1 & 0 & 0 & P_2 \\ 0 & 0 & P_1 & 0 & 0 \\ P_2 & 0 & 0 & P_3 & 0 \\ 0 & P_2 & 0 & 0 & P_3 \end{bmatrix}$$

In which

$$(P_1, P_2, P_3) = \sum_{k=1}^n \int_{z_{k-1}}^{z_k} (\rho)_k (1, z, z^2) dz$$

The element load vector due to hygrothermal forces and moments is given by

$$\{P_e\} = \iint N_i \begin{bmatrix} q \\ 0 \\ 0 \end{bmatrix} dx dy \dots \dots \dots (24)$$

3.6 Solution Process

The stiffness matrix, the initial stress stiffness matrix, the mass matrix and the load vectors of the element, given by equations (19) and (22)-(24), are evaluated by first expressing the integrals in local natural co-ordinates, ξ and η of the element and then performing numerical integration by using Gaussian quadrature. Then the element matrices are assembled to obtain the respective global matrices $[K]$, $[K_G^r]$, $[K_G^a]$, $[M]$, $\{P\}$ and $\{P^N\}$. The first part of the solution is to obtain the initial stress resultants induced by the external transverse static load and by moisture and temperature in static conditions.

$$[K]\{\delta^i\} = \{P\} + \{p^N\} \dots \dots \dots (25)$$

Then the initial stress resultants N_x^i , N_y^i , N_{xy}^i , M_x^i , M_y^i , M_{xy}^i , Q_x^i and Q_y^i are obtained from equations (11) and (18).

The second part of the solution involves determination of natural frequencies from the condition.

$$[K] + [K_G^r] - \omega_n^2 [K_G^a] \{\delta\} = 0$$

Where ω_n = natural frequency

3.7 Computer Program

A computer program is developed by using MATLAB environment to perform all the necessary computations. The element stiffness and mass matrices are derived using a standard procedure. Numerical integration technique by Gaussian quadrature is adopted for the element matrix. Since the stress field is non-uniform, plane stress analysis is carried out using the

finite element techniques to determine the stresses and these stresses are used to formulate the geometric stiffness matrix. The overall matrices $[K_b]$, $[K_g]$, and $[M]$ are obtained by assembling the corresponding element matrices, using skyline technique. The boundary conditions are imposed restraining the generalized displacements in different nodes of the discretized structure.

RESULTS & DISCUSSIONS

4.1 Introduction

The composites plates/shells with arbitrary geometries and boundary conditions subjected to hygrothermal loading got important roles to play as the structural elements in aerospace and other engineering structures. The plate and shell structures subjected to hygrothermal loading cause non-uniform stress field which greatly affects the stability and dynamic behavior of structures.

Here the results of free vibration, buckling & dynamic stability analysis of laminated panels subjected to uniform distribution of moisture and temperature in the absence of external static load are presented using the formulations given above. Here numerical results for free vibration and buckling of laminated composite panels under hygrothermal loadings are presented. In the present case the value of shear correction factor is assumed as 5/6.

4.2 Boundary conditions

Numerical results are presented for laminated composite plates/shells with different combinations of boundary conditions. Shells of various geometry such as cylindrical ($R_y/R_x = 0$), spherical ($R_y/R_x = 1$).

In the discussion that followed S and C denote simply-supported, clamped Edges respectively. For comparison problems, the boundary conditions are considered as reported in the respective studies. Two types of displacement based simply supported boundary conditions are considered in the present study using first order shear deformation theory (FSDT).

The boundary conditions are described as follows:

- (i) Simply supported boundary
S: $u=v=w= \theta_y=0$ at $x=0, a$, and $u=v= w= \theta_x=0$ at $y=0, b$
S₂: $u=w= \theta_y=0$ at $x=0, a$, and $v= w= \theta_x=0$ at $y=0, b$
- (ii) Clamped boundary
C: $u=v=w= \theta_x= \theta_y=0$ at $x=0, a$ and $y=0, b$

The results are presented for symmetric cross-ply and anti-symmetric angle-ply laminated composite plates/shells using “S” simply supported conditions and the comparison with

previous study has been done for frequency of cross-ply laminated composite shells using “S₂” simply supported conditions.

4.3 Non-dimensionalisation of parameters

The non-dimensionalisation of different parameters like vibration, buckling and the excitation frequency for dynamic stability analysis are taken as shown in Table 1 in line with Bert *et al.* (1988), Leissa *et al.* (1988), Moorthy *et al.* (1990).

Table 1: Non-dimensionalisation of parameters

No	Parameter	Plates/Shells
		Composite
1	Frequencies of vibration (ω)	$\bar{\omega}a^2\sqrt{\rho/E_2h^2}$
2	Buckling load (λ)	$N_x b^2/E_2h^3$
3	Frequencies of excitation (Ω)	$\bar{\Omega}a^2\sqrt{\rho/E_2h^2}$

4.4 Vibration, buckling and dynamic stability of panels

- Convergence Study
- Comparison with Previous Studies
- Numerical Results

4.4.1 Convergence study

The convergence study is done for non-dimensional frequencies of free vibration of simply supported and clamped square 4 layer symmetric cross ply and anti-symmetric angle ply laminated composite plates for elevated temperature and moisture conditions for different mesh division as shown in Table 2, 3 and table 4. The study is further extended to buckling analysis of laminated composite plates subjected to hygrothermal condition as presented in Table 5 and 6 and this mesh is employed throughout free vibration, buckling and dynamic stability analysis of laminated composite plates in hygrothermal environment.

Table 2: Convergence of non-dimensional free vibration frequencies for SSSS

4 layer plates for different ply orientations at 325K temperature

$$a/b=1, a/t=100, \text{At } T = 300K, E_1 = 130 \times 10^9, E_2 = 9.5 \times 10^9, G_{12} = 6 \times 10^9$$

$$G_{13} = G_{12}, G_{23} = 0.5G_{12}, \nu_{12} = 0.3, \alpha_1 = -0.3 \times 10^{-6} / ^\circ K, \alpha_2 = 28.1 \times 10^{-6} / ^\circ K$$

$$\text{Non-dimensional frequency, } \lambda = \omega_n a^2 \sqrt{\rho / E_2 t^2}$$

Mesh Division	Non-dimensional frequencies at 325K Temperature	
	(0/90/90/0)	(45/-45/45/-45)
4×4	8.079	11.380
6×6	8.039	10.785
8×8	8.036	10.680
10×10	8.036	10.680

Table3: Convergence of non-dimensional free vibration frequencies for SSSS

4 layer plates for different ply orientations at 0.1%moisture concentration

$$a/b=1, a/t=100, \text{At } C = 0.00, E_1 = 130Gpa, E_2 = 9.5Gpa, G_{12} = 6Gpa$$

$$G_{13} = G_{12}, G_{23} = 0.5G_{12}, \nu_{12} = 0.3, \beta_1 = 0, \beta_2 = 0.44$$

$$\text{Non-dimensional frequency, } \lambda = \omega_n a^2 \sqrt{\rho / E_2 t^2}$$

Mesh Division	Non-dimensional frequencies at C = 0.1%	
	(0/90/90/0)	(45/-45/45/-45)
4×4	9.422	12.3837
6×6	9.387	11.858
8×8	9.384	11.765
10×10	9.384	11.765

Table4: Convergence of non-dimensional free vibration frequencies for CCCC

4 layer plates for different ply orientations at 325 K temperature

$a/b=1, a/t=100, \text{At } T = 300K, E_1 = 128Gpa, E_2 = 9.4Gpa, G_{12} = 6.28Gpa$
 $G_{13} = G_{12}, G_{23} = 0.5G_{12}, \nu_{12} = 0.3, \alpha_1 = -0.3 \times 10^{-6} / ^\circ K, \alpha_2 = 28.1 \times 10^{-6} / ^\circ K$

$$\text{Non-dimensional frequency, } \lambda = \omega_n a^2 \sqrt{\rho / E_2 t^2}$$

Mesh Division	Non-dimensional frequencies at $T = 325K$	
	(0/90/90/0)	(45/-45/45/-45)
4×4	16.666	15.6055
8×8	16.6253	15.5187
10×10	16.6237	15.5147

Table5: Convergence of non-dimensional critical load for SSSS 4 layer plates

for different ply orientations at 325K temperature

$a/b=1, a/t=100, \text{At } T = 300K E_1 = 130Gpa, E_2 = 9.5Gpa, G_{12} = 6Gpa$
 $G_{13} = G_{12}, G_{23} = 0.5G_{12}, \nu_{12} = 0.3, \alpha_1 = -0.3 \times 10^{-6} / ^\circ K, \alpha_2 = 28.1 \times 10^{-6} / ^\circ K$

$$\text{Non-dimensional critical load, } \lambda = \frac{N_{xcr}}{(N_{xcr})_{C=0\%, T=300K}}$$

Mesh Division	Non-dimensional critical load at 325K Temperature	
	(0/90/90/0)	(45/-45/45/-45)
4×4	0.4481	0.6120
6×6	0.4459	0.5818
8×8	0.4457	0.5764
10×10	0.4457	0.5764

Table 6: Convergence of non-dimensional critical load for SSSS 4 layer plates

For different ply orientations at 0.1% moisture concentration

$$a/b=1, a/t=100, \text{ At } T = 300K, E_1 = 130Gpa, E_2 = 9.5Gpa, G_{12} = 6Gpa$$

$$G_{13} = G_{12}, G_{23} = 0.5G_{12}, \nu_{12} = 0.3, \alpha_1 = -0.3 \times 10^{-6} / ^\circ K, \alpha_2 = 28.1 \times 10^{-6} / ^\circ K$$

$$\text{Non-dimensional critical load, } \lambda = \frac{N_{xcr}}{(N_{xcr})_{C=0\%, T=300K}}$$

Mesh Division	Non-dimensional critical load at C=0.1%	
	(0/90/90/0)	(45/-45/45/-45)
4×4	0.6095	0.7255
6×6	0.6079	0.7041
8×8	0.6078	0.7003
10×10	0.6078	0.6990

4.4.2 Comparison with Previous Studies

Numerical computations are carried out to determine the capability of the present isoparametric plate and doubly curved element to predict the dynamic behavior and stability of laminated composite plates. The results obtained by this present formulation are compared with the analytical, independent finite element and/or experimental results published by other investigators wherever possible for variety of problems on plates and shells. Unless otherwise mentioned the mesh division used in the present analysis is 8×8 considering the whole plate/shells for almost all the geometrical configurations, based on convergence studies.

4.4.2.1 Vibration of composite plates and shells subjected to hygrothermal environment

The present formulation is validated for free vibration analysis of composites plates for temperature and moisture as shown in Table 8 & 9. The four lowest non-dimensional frequency parameters due to hygrothermal loadings obtained by the present finite element are compared with numerical solution published by Sairam and Sinha (1992) and with those of

Shen *et al.* (2004) using finite element method. The non-dimensional frequency parameters for plates and shells with normal temperature are compared with analytical solution published by Reddy (1984), Chandrasekhar (1989) as shown in Table 7. The non-dimensional frequency parameters for shell with hygrothermal condition is as shown in Table 10 is compared with results published by Parhi *et al.* (2001) and Naidu & Sinha (2006). The present finite element results show good agreement with the previous numerical results published in the literature for free vibration of laminated composite plates and shells subjected to hygrothermal conditions.

The results obtained by this present formulation are compared with the analytical results published by the other investigators wherever possible for variety of problems on plates and shells under hygrothermal loadings.

Table 7: Comparison of non-dimensional free vibration frequencies for S2 (0/90/90/0) spherical shell at normal temperature

$$a/b=1, a/t=100, \text{ At } T = 300K \quad E_1 = 125Gpa, E_2 = 5Gpa, G_{12} = 2.5Gpa$$

$$G_{13} = G_{12}, G_{23} = 1Gpa, \nu_{12} = 0.25$$

$$\text{Non-dimensional frequency, } \lambda = \omega_n a^2 \sqrt{\rho / E_2 t^2}$$

R/b	Reddy(1984)	Chandrasekhara (1989)	Present
1	126.33	126.7	126.460
2	68.294	68.294	68.364
3	47.415	47.553	47.459
4	37.082	37.184	37.110
5	31.079	31.159	31.097
10	20.38	20.417	20.376
10 ³⁰	15.184	15.195	15.165

Table 8: Comparison of non-dimensional free vibration frequencies for SSSS (0/90/90/0) plates at 325K temperature

$$a/b=1, a/t=100, \text{At } T = 300K \quad E_1 = 130Gpa, E_2 = 9.5Gpa, G_{12} = 6Gpa$$

$$G_{13} = G_{12}, G_{23} = 0.5G_{12}, \nu_{12} = 0.3, \alpha_1 = -0.3 \times 10^{-6} / ^\circ K, \alpha_2 = 28.1 \times 10^{-6} / ^\circ K$$

$$\text{Non-dimensional frequency, } \lambda = \omega_n a^2 \sqrt{\rho / E_2 t^2}$$

Methods	Non-dimensional frequencies at 325K Temperature			
	1	2	3	4
Sairam & Sinha(1991)	8.088	19.196	39.324	45.431
Present FEM	(8.0791)	(19.1002)	(39.3358)	(45.3505)
Patel, Ganapathi & Makhecha(2002)	8.0531	–	–	–
Present FEM	(8.0368)	(18.3398)	(38.4972)	(40.5017)
Hung, Hen & Zheng(2004)	8.043	18.140	38.364	44.686
Present FEM	(8.0791)	(19.1002)	(39.3358)	(45.3505)

Table 9: Comparison of non-dimensional free vibration frequencies for SSSS (0/90/90/0) plate at 0.1% moisture concentration

$$a/b=1, a/t=100, E_1 = 130Gpa, E_2 = 9.5Gpa, G_{12} = 6Gpa$$

$$G_{13} = G_{12}, G_{23} = 0.5G_{12}, \nu_{12} = 0.3, \beta_1 = 0, \beta_2 = 0.44$$

$$\text{Non-dimensional frequency, } \lambda = \omega_n a^2 \sqrt{\rho / E_2 t^2}$$

Methods	Non-dimensional frequencies at C = 0.1%			
	1	2	3	4
Sairam & Sinha(1991)	9.429	20.679	40.068	46.752
Present FEM	(9.4223)	(20.5974)	(40.0842)	(46.7083)
Patel, Ganapathi & Makhecha(2002)	9.3993	–	–	–
Present FEM	(9.3848)	(19.8772)	(39.2529)	(41.9324)
Hung, hen & Zheng(2004)	9.389	19.866	39.265	45.518
Present FEM	(9.4223)	(20.5974)	(40.0842)	(46.7083)

Table 10: Comparison of natural frequencies for S2 (0/90/90/0) shell at 1% moisture concentration

$$a/b=1, a/t=100, E_1 = 172.5Gpa, E_2 = 6.9Gpa (C=0), G_{12} = 3.45Gpa, E_2=6.17Gpa(C=1.0\%)$$

$$G_{13} = G_{12}, G_{23} = 1.38G_{12}, \nu_{12} = 0.25, \beta_1 = 0, \beta_2 = 0.44, \rho=1600$$

$$\text{Fundamental natural frequency, } \lambda = \omega_n a^2 \sqrt{\rho / E_2 t^2} \quad (1/2 * \pi)$$

Stacking sequence	source	C=0	C=1%
R/a=5, (0/90) ₂	Present	201.93	201.61
	Naidu & Sinha(2006)	201.82	201.68
	Parhi <i>et al.</i> (2001)	202.02	201.64
R/a=10, (0/90) ₂	Present	129.08	128.62
	Naidu & Sinha(2006)	129.13	127.54
	Parhi <i>et al.</i> (2001)	129.20	128.32

The present finite element results show good agreement with the previous analytical as well as computational results of other authors. A dash in Table 8 and 9, means in analytical method frequencies for other modes are not available except 1st mode.

4.4.2.2 Buckling of Composite plates subjected to hygrothermal environment

The present formulation is then validated for buckling analysis of laminated composite shells for normal temperatures and moistures. The non-dimensional critical loads due to normal temperature and moisture obtained by the present finite element as shown in Table 12 is compared with analytical solution published by Scuiiva & Carrera (1990). The square plate has four layers of Graphite/Epoxy composite. The non-dimensional critical load due to hygrothermal loadings obtained by the present finite element is compared with numerical solution published by Sairam and Sinha (1992) and Patel, Ganapathi and Makhecha (2002) as shown in Table 11. The present finite element results show good agreement with the previous numerical results published in the literature for buckling of composite plates subjected to hygrothermal loads.

Table 11: Comparison of non-dimensional critical load for SSSS (0/90/90/0) plates at 325K temperature and 0.1% moisture concentration

$a/b=1, a/t=100, \text{At } T = 300K, E_1 = 130Gpa, E_2 = 9.5Gpa, G_{12} = 6Gpa, G_{13} = G_{12}, G_{23} = 0.5G_{12}$
 $, \nu_{12} = 0.3, \alpha_1 = -0.3 \times 10^{-6} / ^\circ K, \alpha_2 = 28.1 \times 10^{-6} / ^\circ K, \beta_1 = 0, \beta_2 = 0.44$

$$\text{Non-dimensional critical load, } \lambda = \frac{N_{xcr}}{(N_{xcr})_{C=0\%, T=300K}}$$

Methods	Non-dimensional critical load λ	
	At T=325K	At C=0.1%
Sairam & Sinha(1991)	0.4488	0.6099
Present FEM	(0.4481)	(0.6095)
Patel, Ganapathi & Makhecha(2002)	0.4466	0.6084
Present FEM	(0.4457)	(0.6078)

Table 12: Comparison of Non-dimensional buckling loads of a square simply supported symmetric cross-ply cylindrical laminated curved panels with (0/90/0/90/0)

$a/b=1, R/a=20.0, \lambda=N_x a^2/E_2 h^3, E_{11}=40E_{22}, G_{23}=0.6E_2, G_{12}=G_{13}=0.5E_{22}, \nu_{12}=\nu_{13}=0.25$

Theory	a/h=50	a/h=100
Present work	35.235	36.8030
FSDT(Scuiiva & Carrera)(1990)	35.42	36.843

There exists an excellent agreement between the present FEM and the previously published results of other authors.

4.4.3 Numerical Results

After obtaining the convergence study and validating the formulation with the existing literature, the results for vibration, buckling and dynamic stability studies for the plate subjected to temperature and moisture are presented. The material properties used for the numerical study:

At $T = 300K$ $E_1 = 130Gpa$, $E_2 = 9.5Gpa$, $G_{12} = 6Gpa$, $G_{13} = G_{12}$, $G_{23} = 0.5G_{12}$, $\nu_{12} = 0.3$,
 $\alpha_1 = -0.3 \times 10^{-6} / ^\circ K$, $\alpha_2 = 28.1 \times 10^{-6} / ^\circ K$, $\beta_1 = 0$, $\beta_2 = 0.44$

4.4.3 Numerical Results for Vibration and buckling

The result for vibration & buckling has been studied with variation of temperature and moisture.

4.4.3.1 Effects of Temperature on Frequencies of Vibration:

The variation of non-dimensional frequency parameter $\lambda = \omega_n a^2 \sqrt{\rho / E_2 t^2}$ for a four layer simply-supported laminated composite plate subjected to uniform distribution of temperature from 300K to 350K is shown in fig.5.

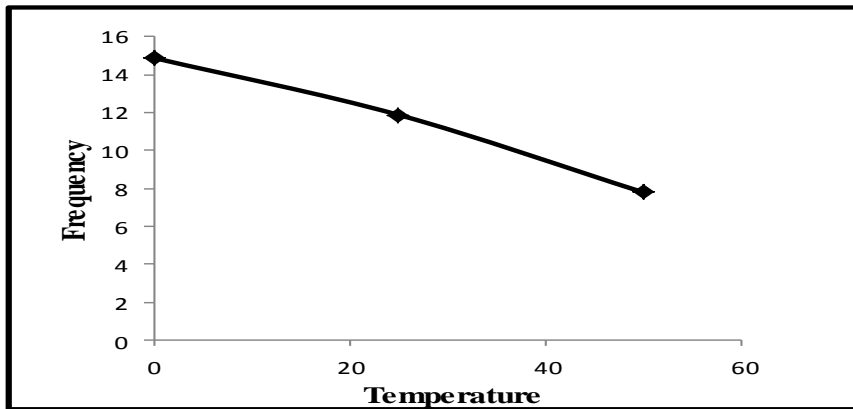


Fig 5: Effect of temperature on non-dimensional frequency of (45/-45/45/-45) laminate

(a/b=1, b/t=100)

In fig 5, it is shown that the fundamental natural frequency decreases with increasing in temperature. It is shown that the reduction in fundamental frequency with increase in temperature may be linear or non-linear depending upon the temperature, but the percentage of reduction of fundamental frequency with increasing in temperature is more for both symmetric and anti-symmetric cross-ply laminates in comparison to symmetric and anti-symmetric angle-ply laminates.

4.4.3.2 Effects of Moisture Concentration on Frequencies of Vibration:

The variation of non-dimensional frequency parameter $\lambda = \omega_n a^2 \sqrt{\rho / E_2 t^2}$ for a four layer simply-supported laminated composite plate, subjected to uniform distribution of moisture concentration from 0% to 0.25% is shown in fig. 6.

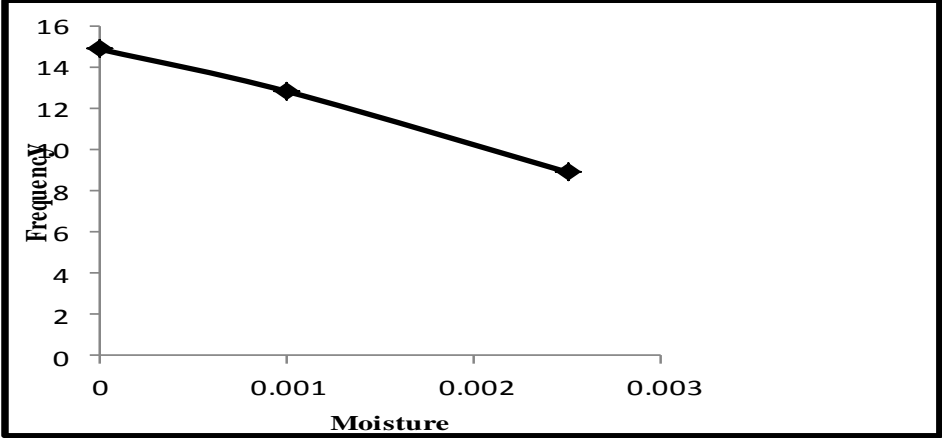


Fig.6: Effect of moisture on non-dimensional frequency of (45/-45/45/-45) laminate

As observed in fig.6, the reduction in fundamental frequency with increase in moisture concentration may be linear or non-linear depending upon the moisture concentration, but the percentage of reduction of fundamental frequency with increasing in moisture concentration is more for both symmetric and anti-symmetric cross-ply laminates in comparison to angle-ply symmetric and anti-symmetric laminates.

4.4.3.3 Effects of Temperature on Critical Load

The variation of non-dimensional critical load $\lambda = N_{xcr} / (N_{xcr})_{C=0\%, T=300K}$ for a four layer simply-supported laminated composite plate, subjected to uniform distribution of temperature from 300K to 350K with different ply orientations is shown in fig 7. It is shown that the reduction in critical loads with increasing in uniform temperature is of the same order for cross-ply symmetric and anti-symmetric laminates. For angle-ply symmetric and anti-symmetric laminates it is also true. With increase in temperature the reduction of critical loads is non-linear.

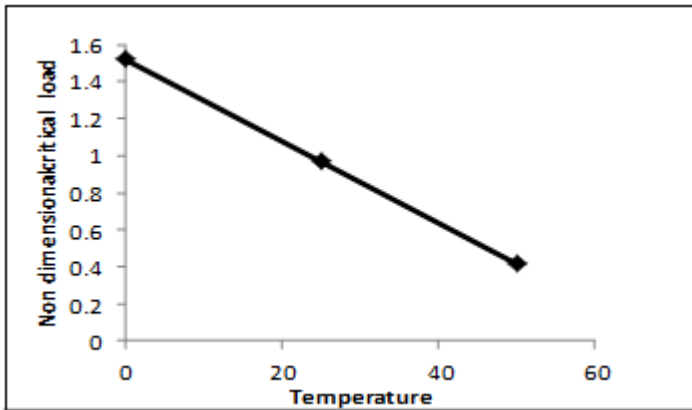


Fig.7: Effect of temperature on non-dimensional critical load of angle-ply laminate

4.4.3.4 Effects of Moisture Concentration on Critical Load

The variation of non-dimensional critical load $\lambda = \frac{N_{xcr}}{(N_{xcr})_{C=0\%,T=300K}}$ for a four layer simply-supported composite plate ($a/b=1$, $b/t=100$), subjected to uniform distribution of moisture concentration from 0% to 0.25% with different ply orientations is shown in fig. 8.

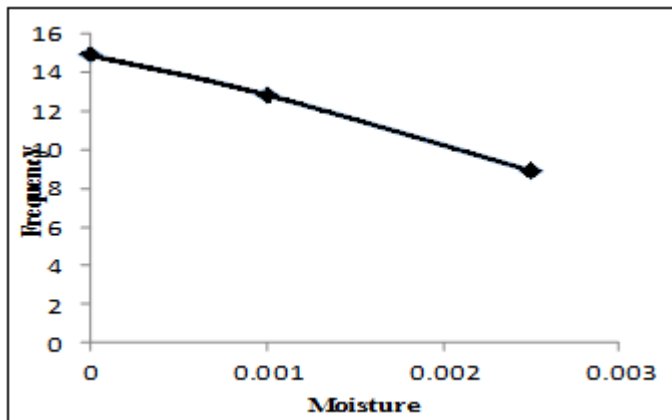


Fig.8: Effect of moisture on non-dimensional critical load of angle-ply laminate

In fig 8, it is shown that the reduction in critical loads with increasing in uniform moisture concentration is of the same order for cross-ply symmetric and anti-symmetric laminates. For angle-ply symmetric and anti-symmetric laminates it is also true. With increase in uniform moisture concentration the reduction of critical loads is nearly linear.

4.5 Numerical Results for Dynamic stability of Laminated Composite Plates

After validating the present formulation, the same is employed to study the dynamic stability effects of laminated composite plates in hygrothermal environment. Numerical Results are

presented on the dynamic stability of cross-ply and angle-ply laminated plate to study the effects of various parameters on instability regions. The geometrical properties of the laminated plate are as follows:

$a=500\text{mm}$, $b=500\text{mm}$, $t=5\text{mm}$, $E_1=130\text{Gpa}$, $E_2=9.5\text{Gpa}$, $G_{12}=6\text{Gpa}$, $G_{23}/G_{12}=0.5$, $\nu_{12}=0.3$, $G_{13}=G_{12}$, $\alpha_1=-0.3*10^{-6}/\text{K}$, $\alpha_2=28.1*10^{-6}/\text{K}$, $\text{Temp}=0\text{K}$

Dynamic instability regions (DIR) are plotted in the plane having load frequency (Ω/ω) as abscissa and load amplitude ($\beta=N_t/N_{cr}$) as ordinate. The non-dimensional excitation frequency $\Omega=\bar{\Omega}a^2\sqrt{(\rho/E_2h^2)}$ is used throughout the dynamic instability studies, where $\bar{\Omega}$ is the excitation frequency in radian/sec. The principal instability regions of laminated composite flat panel subjected to in-plane periodic loads is plotted with non-dimensional frequency Ω/ω (ratio of excitation frequency to the free vibration frequency) versus the dynamic in-plane load β . The analysis is focused on the determination of the primary instability regions of laminated composite plates under hygrothermal loads. The width of primary instability is the separation of the boundaries of the primary instability regions for the given plate. This can be used as an instability measure to study the influence of the other parameters. This is the most dangerous zone and has the greatest practical importance.

4.5.1 Effect of static load factor on instability regions of uniformly loaded symmetric plate

The effect of static load factor on instability of laminated composite plate subjected to hygrothermal condition is shown in fig.9. It is observed that with the increase of static load factor from 0 to 0.4, the onset of dynamic instability occurs earlier and the width of dynamic instability region (DIR) also increases. All further studies are made with a static load factor of 0.2 (unless otherwise mentioned).

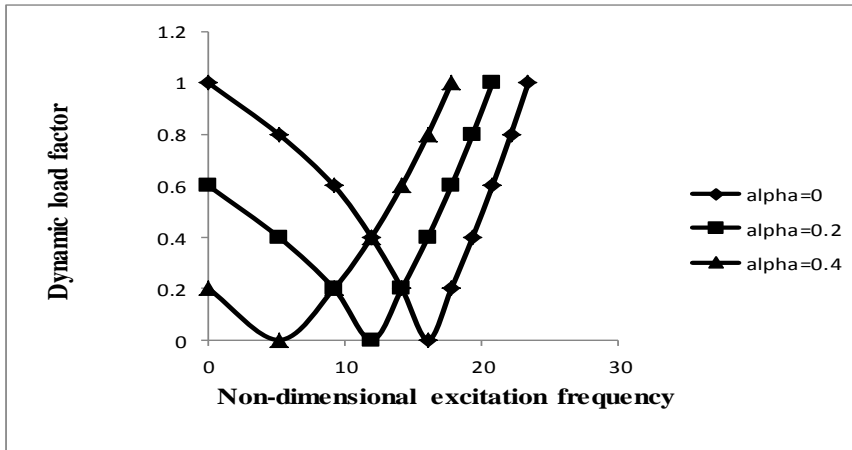


Fig9: Variations of instability region with static load factor of composite symmetric laminated plate subjected to hygrothermal loading

4.5.2 Effects of Temperature on excitation frequency:

The variation of excitation frequency with dynamic load factor of composite laminated simply-supported symmetric cross-ply square plates subjected to uniform distribution of temperature of 300K and 325K is shown in fig.10. It is observed that the onset of instability occurs earlier with wider DIR for symmetric cross-ply laminated composite plates subjected to elevated temperature compared to composite plates with normal temperature. With increase in temperature from 300K to 325K, the excitation frequency is reducing by 44.56%. The width of instability region of laminated plate subjected to elevated temperature is increased by 84% from plate with normal temperature for a dynamic load factor of 0.2.

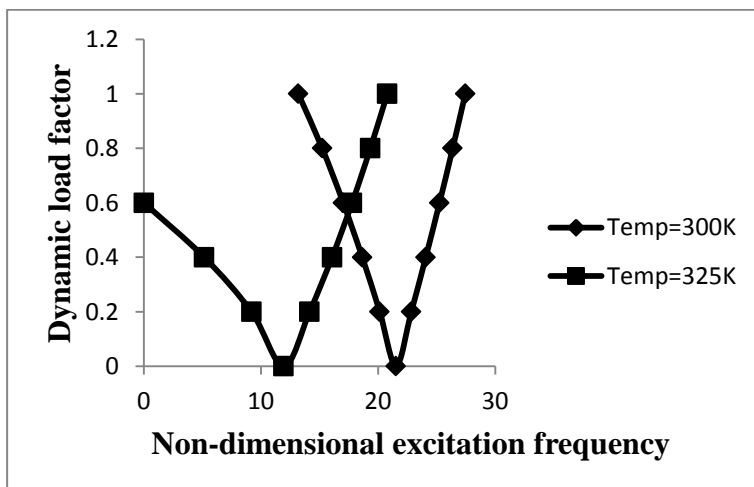


Fig10: Variations of instability region with temperature for composite laminated symmetric cross-ply (0/90/90/0) plate (a/b=1, a/t=100)

The variation of excitation frequency with dynamic load factor of composite laminated simply-supported anti-symmetric angle-ply square plates subjected to uniform distribution of temperature from 300K, 325K & 350K is shown in fig.11. As shown, the onset of instability occurs earlier with wider DIR for anti-symmetric angle-ply laminated composite plate subjected to elevated temperature compared to composite plates with normal temperature. With increase in temperature from 300K to 350K, the excitation frequency is reducing by 59.42%. The width of instability region of laminated plate subjected to elevated temperature 350K is increased by 2.53 times of the plate with normal temperature for a dynamic load factor of 0.2.

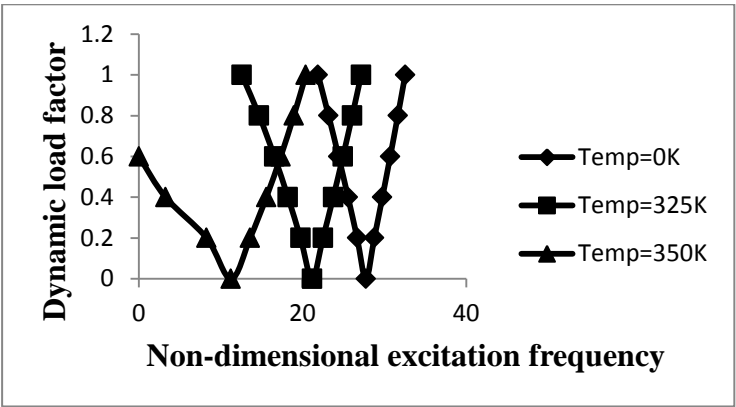


Fig11: Variations of instability region with temperature of composite laminated anti-symmetric angle-ply (45/-45/45/-45) plate

The variation of excitation frequency with dynamic load factor of composite laminated clamped symmetric cross-ply square plate subjected to uniform distribution of temperature from 300K and 325K is shown in fig.12. It is revealed that the onset of instability occurs earlier with wider DIR for symmetric cross-ply laminated composite plate subjected to elevated temperature compared to composite plates with normal temperature. The excitation frequency is reducing by 8.65% by increase in temperature from 300K to 325K. The instability occurs at a higher excitation frequency from simply supported to clamped edges due to the restraint at the edges. The width of the instability regions are also decreased with the increase of restraint at the edges.

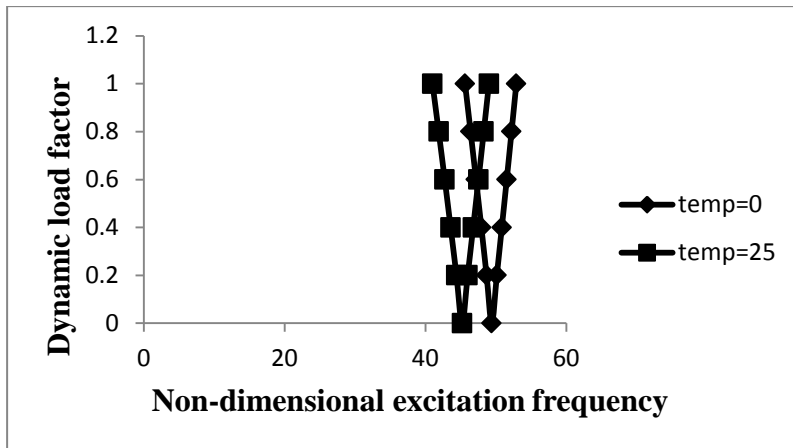


Fig12: Variations of instability region with temperature of composite laminated CCCC symmetric cross-ply (0/90/90/0) plate

4.5.3 Effects of moisture on excitation frequency:

The variation of excitation frequency with dynamic load factor of composite laminated simply-supported symmetric cross-ply square plate subjected to uniform distribution of moisture concentration from 0% & 0.1% is shown in fig.13. It is revealed that the onset of instability occurs earlier with wider DIR for symmetric cross-ply laminated composite plate subjected to elevated moisture condition compared to composite plates with normal moisture. When moisture concentration is increased from 0% to 0.1% then excitation frequency drop is happened for about 28.65%. The width of instability region for laminated plate with elevated temperature is increased by 40.6% from the plate with normal temperature for a dynamic load factor of 0.2.

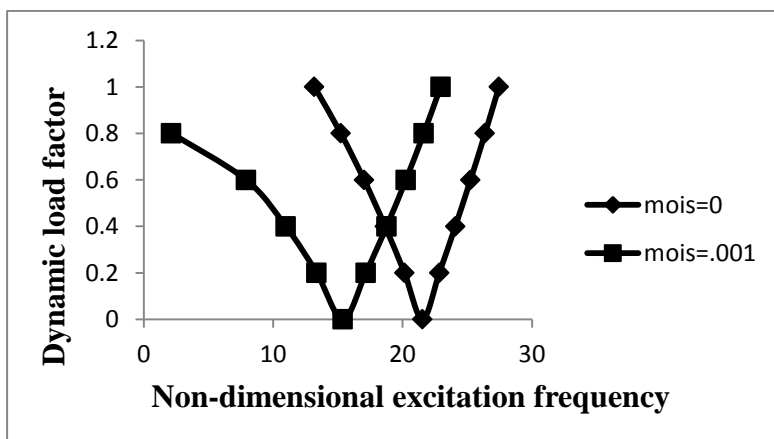


Fig13: Variations of instability region with moisture of composite laminated symmetric cross-ply (0/90/90/0) plate

The variation of excitation frequency with dynamic load factor of composite laminated simply-supported anti-symmetric angle-ply square plate subjected to uniform distribution of moisture concentration from 0%, 0.1% & 0.25% is shown in fig.14. It is revealed that the onset of instability occurs earlier with wider DIR for anti-symmetric angle-ply laminated composite plates subjected to elevated moisture condition compared to composite plates with normal moisture concentration. When moisture concentration is increased from 0% to 0.25% then excitation frequency drop is happened for about 44.58%. The width of instability region for laminated plate with elevated moisture Of 0.25% is increased by 56% from the plate with normal moisture for a dynamic load factor of 0.2.

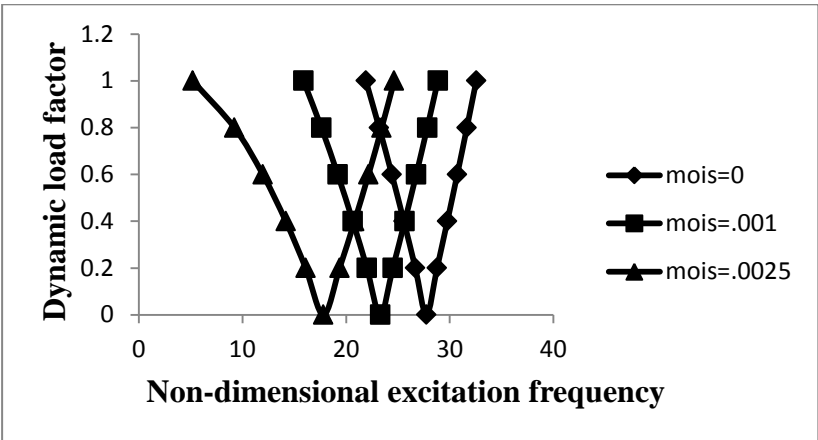


Fig14: Variations of instability region with moisture of composite laminated anti-symmetric angle-ply (45/-45/45/-45) plate

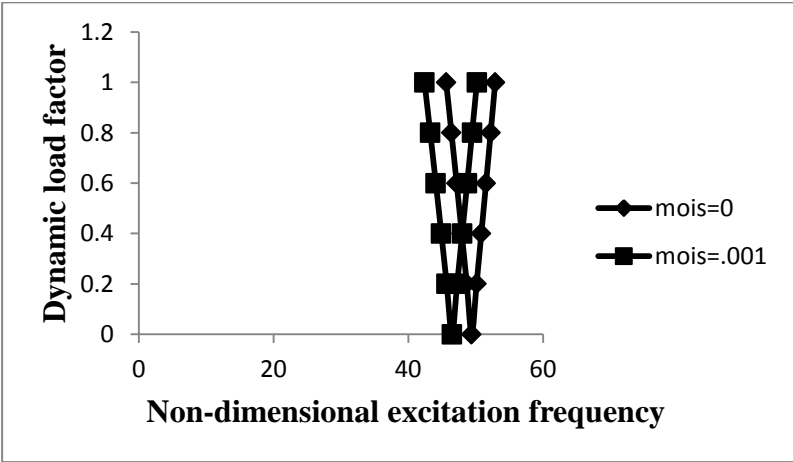


Fig15: Variations of instability region with moisture of composite laminated CCCC symmetric cross-ply (0/90/90/0) plate

The variation of excitation frequency with dynamic load factor of composite laminated clamped symmetric cross-ply square plates subjected to uniform distribution of moisture concentration from 0% & 0.1% is shown in fig.15. As shown the onset of instability occurs

earlier with wider DIR for symmetric cross-ply laminated composite plates subjected to elevated moisture condition compared to composite plates with normal moisture. When moisture concentration is increased from 0% to 0.1% then excitation frequency drop is happened for about 5.93%. The instability occurs at a higher excitation frequency from simply supported to clamped edges due to the restraint at the edges. The width of the instability regions are also decreased with the increase of restraint at the edges.

4.5.4 Effects of Aspect Ratio on excitation frequency

The variation of excitation frequency with dynamic load factor of composite laminated simply-supported anti-symmetric angle-ply square plates subjected to uniform distribution of temperature with different aspect ratio($a/b = 1, 2 \text{ \& } 3$) is shown in fig. 16 .

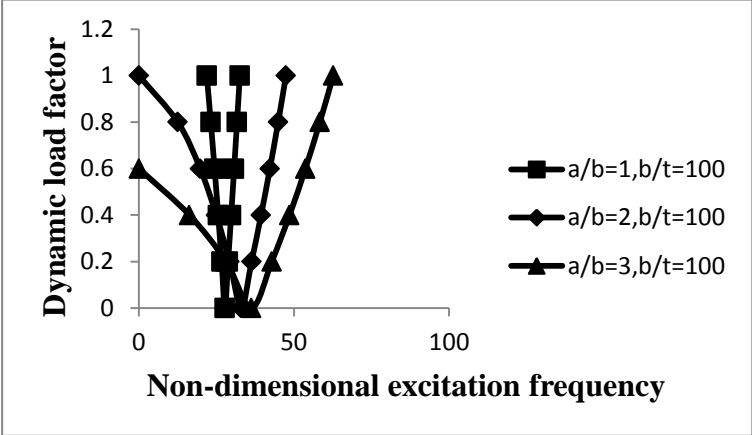


Fig.16: Effect of aspect ratio on instability region of (45/-45/45/-45) laminate with elevated temperature

The study reveals that the onset of instability occurs earlier for anti-symmetric angle-ply laminated composite square plates than rectangular plates subjected to uniform distribution of temperature. However the width of DIR is narrower for square plates in comparison with rectangular plates. The width of instability regions increased marginally for rectangular plates than square plates with uniform rise in temperature. The increase in aspect ratio shifts the frequency of instability region to higher values and reduces the dynamic stability strength. As a result the plates having higher values of aspect ratios are dynamically unstable in elevated temperature and lose its stiffness.

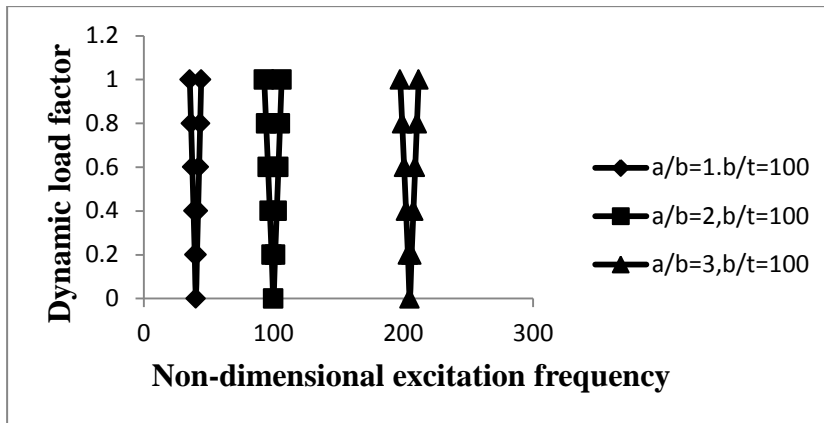


Fig.17: Effect of aspect ratio on instability region of CCCC anti symmetric angle-ply (45/-45/45/-45) laminate with elevated temperature

The variation of excitation frequency with dynamic load factor of composite laminated clamped anti-symmetric angle-ply square plate subjected to uniform distribution of temperature with different aspect ratio ($a/b = 1, 2$ & 3) is shown in fig. 17. As shown the onset of instability occurs earlier for anti-symmetric angle-ply laminated composite square plates than rectangular plates subjected to elevated temperature. However the width of DIR is narrower for square plates in comparison with rectangular plates. The plate is unstable for a wide range of excitation frequencies, due to overlapping of different instability regions associated with lower frequencies.

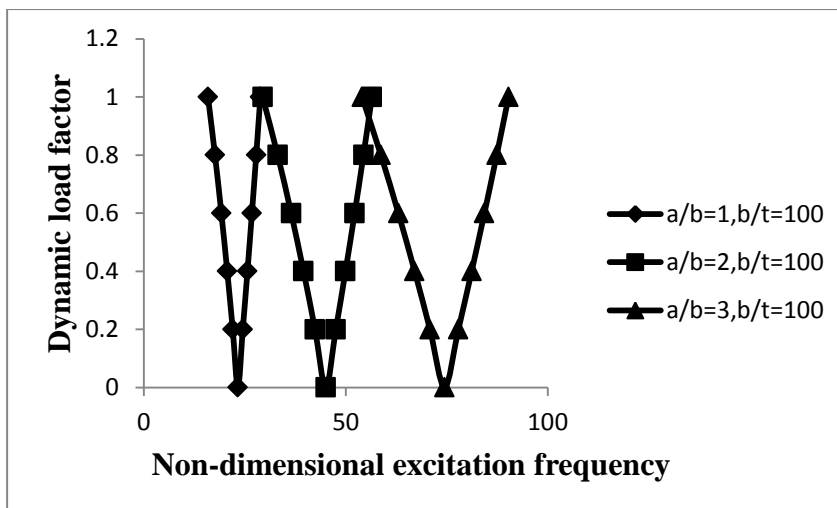


Fig.18: Effect of aspect ratio on instability region of CCCC anti symmetric angle-ply (45/-45/45/-45) laminate with elevated moisture

The variation of excitation frequency with dynamic load factor of composite laminated clamped anti-symmetric angle-ply square plate subjected to uniform distribution of moisture with different aspect ratio ($a/b = 1, 2$ & 3) is shown in fig. 18. It is observed that for anti-

symmetric angle-ply laminated composite square plates the onset of instability occurs earlier than rectangular plates subjected to elevated moisture condition. However the width of DIR is narrower for square plates in comparison with rectangular plates. The width of instability regions increased marginally for rectangular plates than square plates with uniform rise in moisture concentration. The increase in aspect ratio shifts the frequency of instability region to higher values and reduces the dynamic stability strength. As a result the plates having higher values of aspect ratios are dynamically unstable in elevated moisture concentration and lose its stiffness.

4.5.5 Effects of Ply orientation on excitation frequency

The variation of instability region with dynamic load factor of composite laminated simply supported anti-symmetric angle-ply plates with excitation frequency subjected to uniform distribution of temperature with different ply orientation is shown in fig.19.

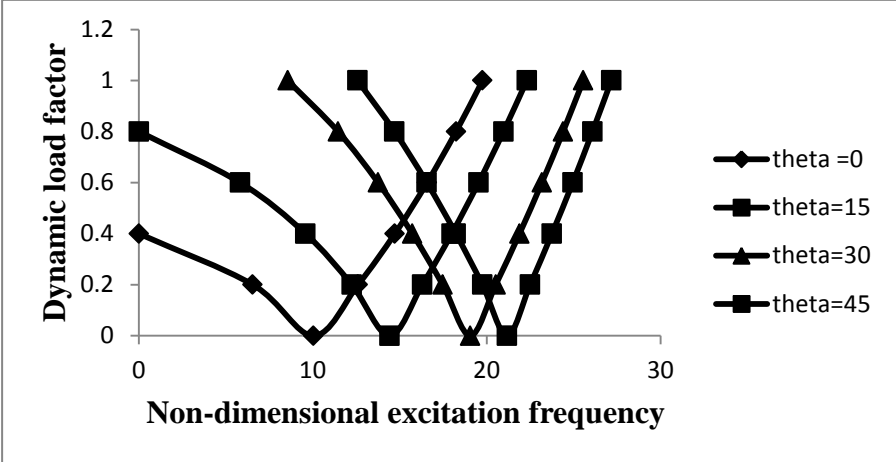


Fig.19: Effect of different ply orientation on instability region of anti-symmetric angle-ply laminate for elevated temperature

From the fig. it is observed that the onset of instability occurs earlier for anti-symmetric angle-ply laminated composite plates with 0 degree of ply orientation than the plates with higher degree of ply orientation subjected to elevated temperature but with wide DIR. The value of ply orientation for which the instability region is narrower is 45 and for the wider DIR the ply orientation value is 0. The greater the lamination angle, the smaller is the instability region. The ply orientation for 0° seems to be the preferential ply orientation for the lamination sequence which is due to dominance effect of bending-stretching coupling.

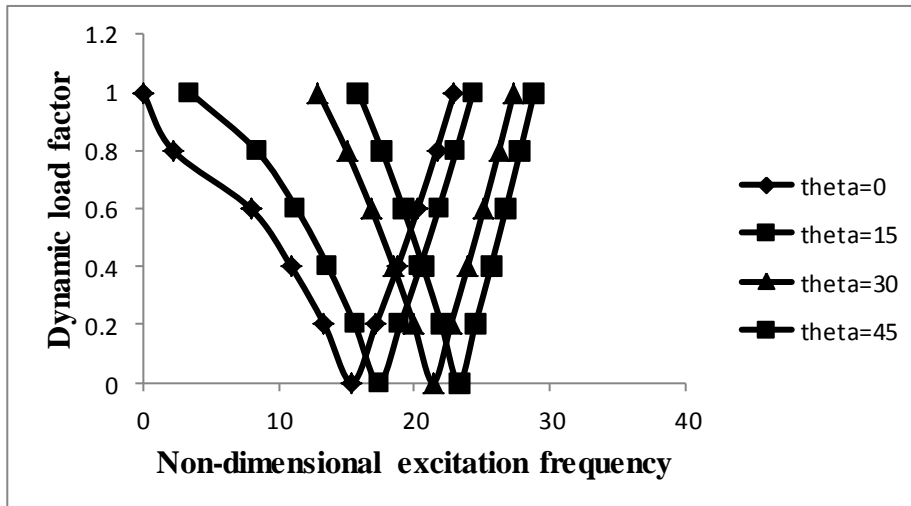


Fig.20: Effect of different ply orientation on instability region of anti-symmetric angle-ply laminate for elevated moisture

The variation of instability region with dynamic load factor of composite laminated simply supported anti-symmetric angle-ply with excitation frequency subjected to uniform distribution of moisture with different ply orientation is shown in fig. 20. It is observed that the onset of instability occurs earlier for anti-symmetric angle-ply laminated composite plates with 0 degree of ply orientation than the plates with higher degree of ply orientation subjected to elevated moisture condition but with wide DIR. The value of ply orientation for which the instability region is narrower is 45 and for the wider DIR the ply orientation value is 0. The instability region is less wide for increase in lamination angle but the excitation frequencies are decreased with decrease in ply-orientation with uniform distribution of moisture concentration.

4.5.6 Effect of temperature & moisture on instability region

The variation of instability region with dynamic load factor of composite laminated simply supported anti-symmetric angle-ply plates with excitation frequency subjected to uniform distribution of temperature and moisture is shown in fig. 21. As shown, the onset of instability occurs latter for anti-symmetric angle-ply laminated composite plates with normal temperature & moisture than plates subjected to hygrothermal condition but with narrower instability regions.

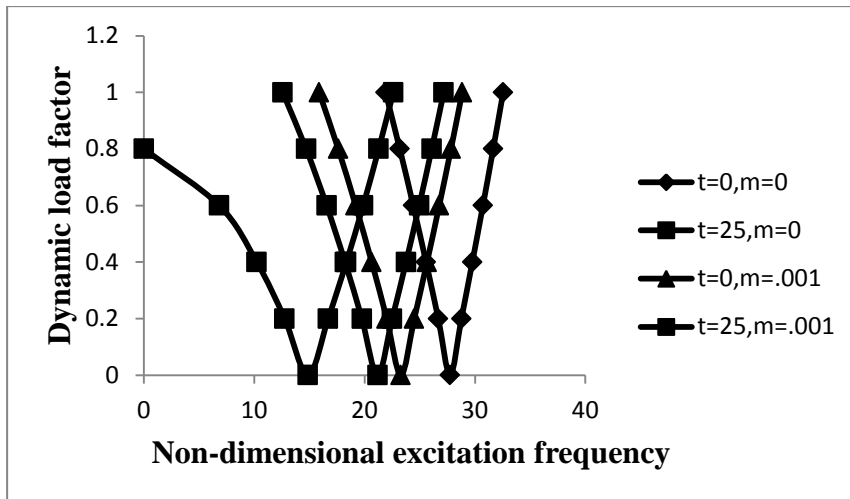


Fig.21: Effect of temperature & moisture on instability region of laminated SSSS anti-symmetric angle-ply (45/-45/45/-45) laminate

The variation of instability region with dynamic load factor of composite laminated clamped anti-symmetric angle-ply with excitation frequency subjected to uniform distribution of temperature and moisture is shown in fig. 22.

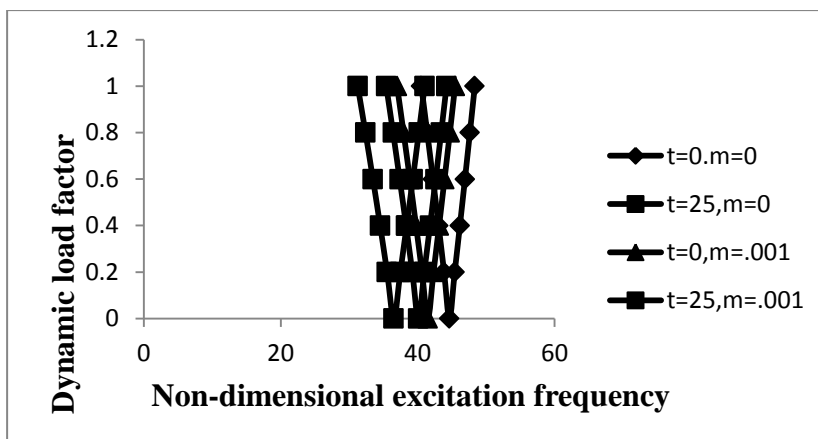


Fig.22: Effect of temperature & moisture on instability region of laminated CCCC anti-symmetric angle-ply (45 -45 45 -45) laminate

As shown the onset of instability occurs latter for anti-symmetric angle-ply laminated composite plates with normal temperature & moisture than plates subjected to hygrothermal condition but with narrow instability regions. The instability occurs at a higher excitation frequency from simply supported to clamped edges due to the restraint at the edges.

4.5.7 Effects of Degree of orthotropy on excitation frequency

The variation of excitation frequency with dynamic load factor of composite laminated simply supported anti-symmetric angle-ply square plates subjected to uniform distribution of temperature is shown in fig. 23. The effect of degree of orthotropy is studied for $E_1/E_2 = 40, 20, 10$, keeping other material properties constant.

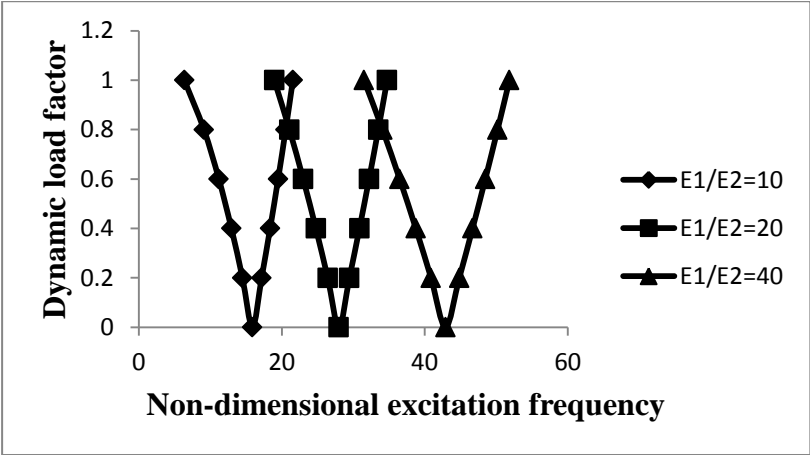


Fig.23: Effect of degrees of orthotropy on instability region of anti-symmetric angle-ply laminate for elevated temperature

It is revealed that the onset of instability occurs latter with increase of degree of orthotropy for anti-symmetric angle-ply laminated composite plates subjected to elevated temperature but with wider instability regions in comparison to plates having lower degree of orthotropy. The excitation frequency reduces by 62.9% for the plate having higher degree of orthotropy to lower degree of orthotropy.

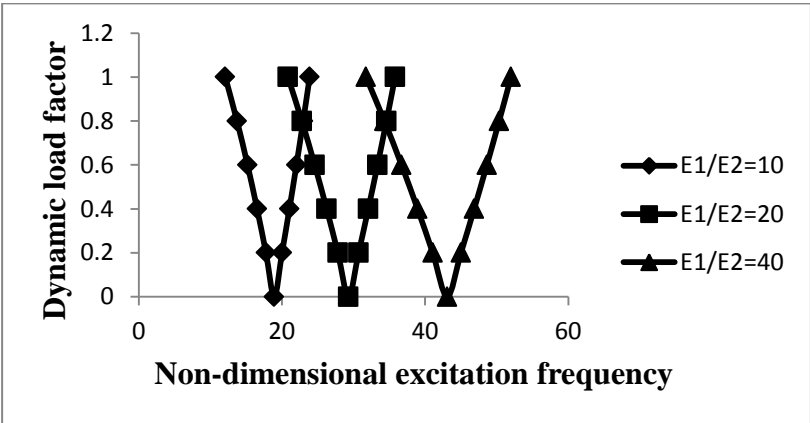


Fig.24: Effect of degrees of orthotropy on instability region of anti-symmetric angle-ply laminate for elevated moisture

The variation of excitation frequency with dynamic load factor of composite laminated simply supported anti-symmetric angle-ply square plates subjected to elevated moisture is shown in fig. 24. The effect of degree of orthotropy is studied for $E_1/E_2 = 40, 20, 10$, keeping other

material properties constant. As shown the onset of instability occurs latter with increase of degree of orthotropy for anti-symmetric angle-ply laminated composite plates subjected to elevated moisture concentration but with wider instability regions compared with plates with ambient moisture concentration. The excitation frequency reduces by 56% for the plate having higher degree of orthotropy to lower degree of orthotropy.

4.5.8 Effect of side to thickness ratio

The variation of excitation frequency with dynamic load factor of composite laminated simply supported anti-symmetric angle-ply plates subjected to uniform distribution of temperature are shown in fig.25. The effect of side to thickness ratio is studied for $b/t = 25$ and 50 . As seen from the fig., the dynamic instability region is less for plate having less side to thickness ratio. As a whole the excitation frequencies are decreased with increase in temperature.

The thicker plates having narrow instability region shows more stiffness and strength than thinner plate in elevated temperature. The width of instability regions increases due to increase in both static and dynamic loads.

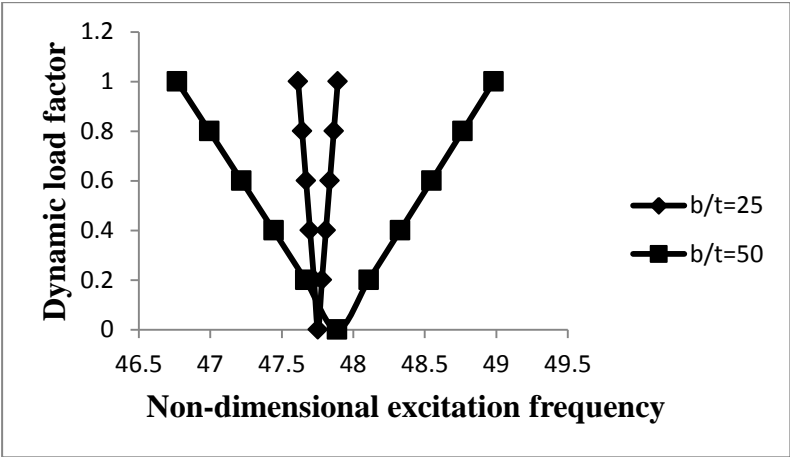


Fig.25 Effect of b/h ratio on instability region of (45/-45/45/-45) laminate for elevated temperature

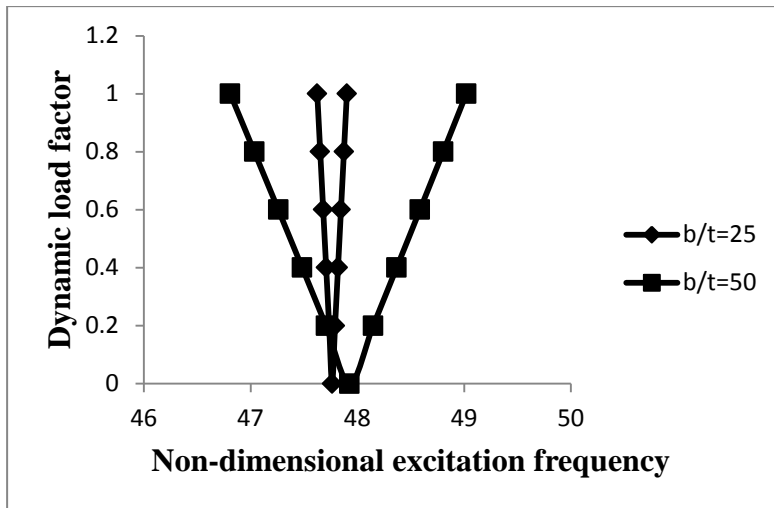


Fig.26 Effect of b/h ratio on instability region of (45/-45/45/-45) laminate for elevated moisture

The effect of side to thickness ratio of anti-symmetric angle-ply composite laminate subjected to elevated temperature is studied for $b/t = 25$ and 50 in fig.26. It is revealed that the dynamic instability region is less for plate having less side to thickness ratio. As a whole the excitation frequencies are decreased with increase in moisture. The thicker plates having narrow instability region shows more stiffness and strength than thinner plate in elevated moisture. The width of instability regions increases due to increase in both static and dynamic loads.

4.5.9 Effects of Boundary condition

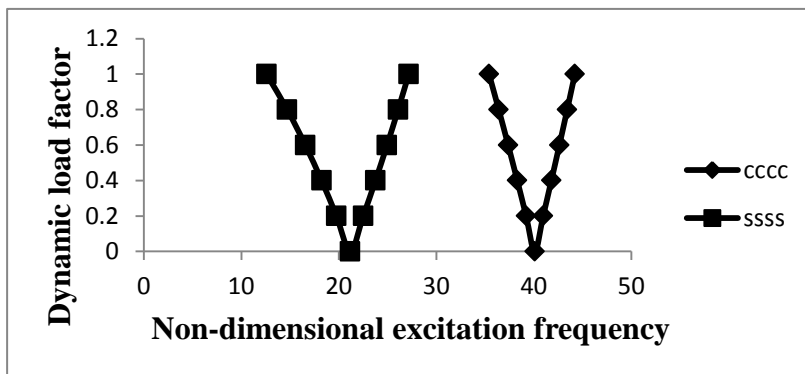


Fig.27: Effect of different boundary condition on instability region of anti-symmetric angle-ply laminate with elevated temperature.

Fig.27 shows the influence of different boundaries (SSSS, CCCC) on the principal instability regions. The instability occurs at a higher excitation frequency from simply supported to clamped edges due to the restraint at the edges. The width of the instability regions are also decreased with the increase of restraint at the edges. The excitation frequency reduces 47% for simply-supported composite angle-ply anti-symmetric laminated plates with elevated

temperature. The width of instability region for simply-supported laminated plate with elevated temperature is increased by 57% from the clamped plate with elevated temperature for a dynamic load factor of 0.2.

4.6 Numerical Results For Dynamic stability of shells

After validating the formulation, the same is employed to study the dynamic stability effects of laminated composite shells in hygrothermal environment. Numerical Results are presented on the dynamic stability of cross-ply and angle-ply laminated shell to study the effects of various parameters on instability regions. The geometrical properties of the laminated shell are as follows:

$a=500\text{mm}$, $b=500\text{mm}$, $t=5\text{mm}$, $E_1=130\text{Gpa}$, $E_2=9.5\text{Gpa}$, $G_{12}=6\text{Gpa}$, $G_{23}/G_{12}=0.5$, $\nu_{12}=0.3$, $G_{13}=G_{12}$, $\alpha_1=-0.3 \cdot 10^{-6} / \text{K}$, $\alpha_2=28.1 \cdot 10^{-6} / \text{K}$, $\text{Temp}=0\text{K}$.

The non-dimensional excitation frequency $\Omega = \bar{\Omega} a^2 \sqrt{(\rho/E_{22}h^2)}$ is used throughout the dynamic instability studies, where $\bar{\Omega}$ is the excitation frequency in radian/sec. The principal instability regions of laminated composite curved panel subjected to in-plane periodic loads is plotted with non-dimensional frequency Ω/ω (ratio of excitation frequency to the free vibration frequency) versus the dynamic in-plane load β . The analysis is focused on the determination of the primary instability regions of laminated composite shells under hygrothermal loads.

4.6.1 Effect of static load factor on instability regions of uniformly loaded symmetric shell

The effect of static component of load for $\alpha = 0.0, 0.2, 0.4, 0.6, 0.8$ and 1 on the instability region is shown in fig.28. Due to increase of static component, the instability regions tend to shift to lower frequencies and become wider. All further studies are made with a static load factor of 0.2 (unless otherwise mentioned).

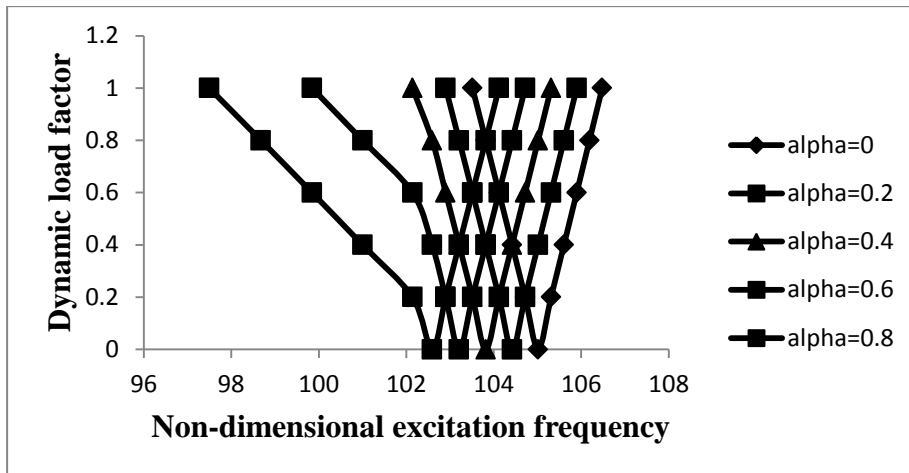


Fig28: Variations of instability region with static load factor of composite symmetric laminated shell subjected to hygrothermal loading

4.6.2 Effects of Temperature on excitation frequency:

The variation of excitation frequency with dynamic load factor of composite laminated simply-supported symmetric cross-ply square shells subjected to uniform distribution of temperature from 300K and 325K is shown in fig.29. It is observed that the onset of instability occurs earlier with wider DIR for symmetric cross-ply laminated composite plates subjected to elevated temperature compared to composite plates with normal temperature. With increase in temperature from 300K to 325K, the excitation frequency is reducing by 31.6%. The width of instability region for laminated plate with elevated temperature is increased by 46.67% from the plate with normal temperature for a dynamic load factor of 0.6.

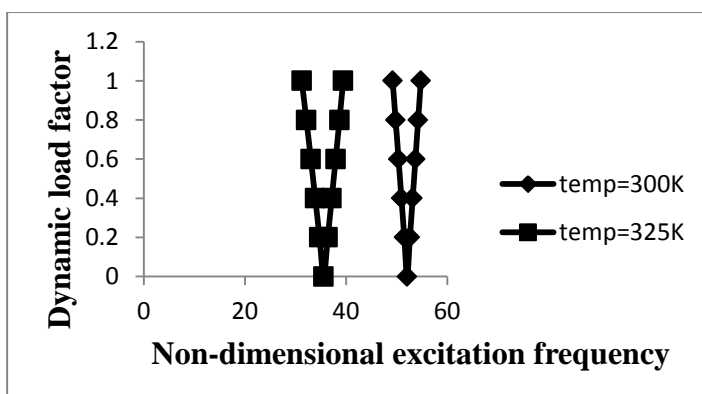


Fig29: Variations of instability region with temperature of composite laminated symmetric cross-ply (0/90/90/0) curved panel

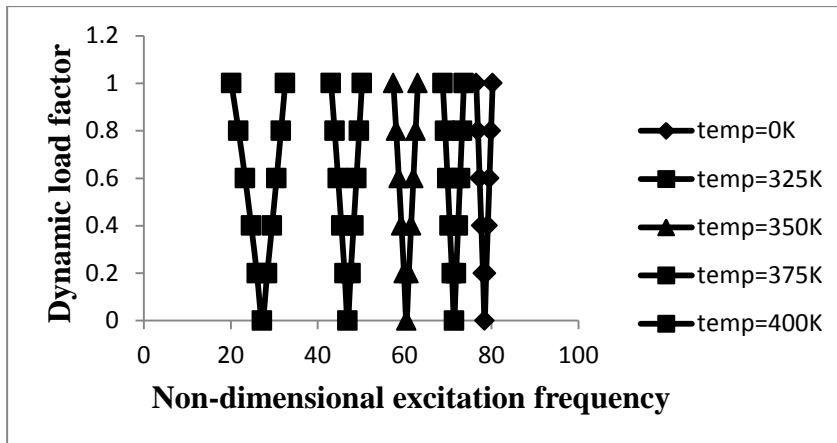


Fig30: Variations of instability region with temperature of composite laminated antisymmetric angle-ply (45/-45/45/-45) curved panel

The variation of excitation frequency with dynamic load factor of composite laminated simply-supported anti-symmetric angle-ply square shells subjected to uniform distribution of temperature from 300K, 325K, 350K, 375K & 400K is shown in fig.30. As shown, the onset of instability occurs earlier with wider DIR for anti-symmetric angle-ply laminated composite shells subjected to elevated temperature compared to composite shells with normal temperature. With increase in temperature from 300K to 350K, the excitation frequency is reducing by 65.2%.

4.6.3 Effects of moisture on excitation frequency:

The variation of excitation frequency with dynamic load factor of composite laminated simply-supported symmetric cross-ply curved panel subjected to uniform distribution of moisture concentration from 0% & 0.1% is shown in fig.31. It is revealed that the onset of instability occurs earlier with wider DIR for symmetric cross-ply laminated composite shells subjected to elevated moisture condition compared to composite shells with normal moisture. When moisture concentration is increased from 0% to 0.1% then excitation frequency drop is happened for about 21%. The width of instability region for laminated shell with elevated temperature is increased by 46.67% from the shell with normal temperature for a dynamic load factor of 0.6.

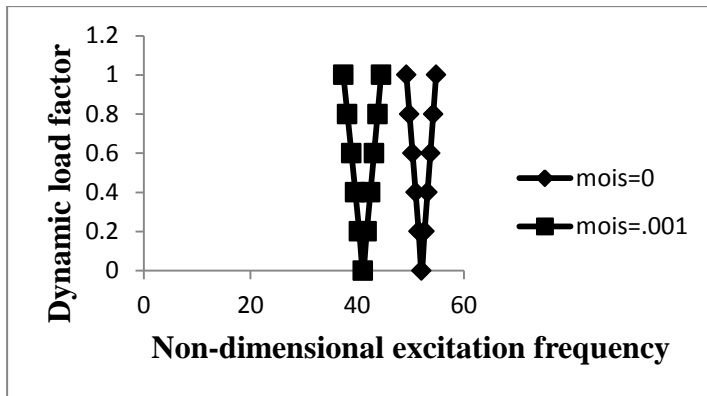


Fig31: Variations of instability region with moisture of composite laminated symmetric cross-ply (0/90/90/0) shell

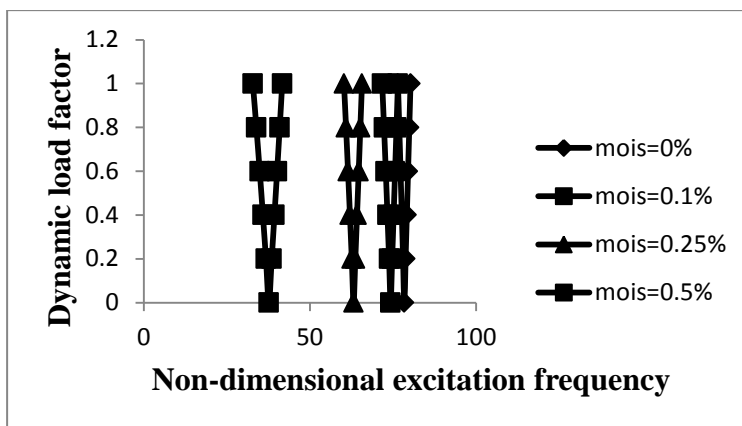


Fig32: Variations of instability region with moisture of composite laminated anti-symmetric angle-ply (45/-45/45/-45) shell

The variation of excitation frequency with dynamic load factor of composite laminated simply-supported anti-symmetric angle-ply shell subjected to uniform distribution of moisture concentration from 0%, 0.1%, 0.25% & 0.5% is shown in fig.32. It is revealed that the onset of instability occurs earlier with wider DIR for anti-symmetric angle-ply laminated composite shells subjected to elevated moisture condition compared to composite shells with normal moisture concentration. When moisture concentration is increased from 0% to 0.25% then excitation frequency drop is happened for about 49.3%.

4.6.4 Effects of curvature on excitation frequency

Studies have also been made (Fig.33) for comparison of instability regions for different shell geometries. The effect of curvature on instability region of different curved panels for $a/b=1$, flat panel ($a/R_x = b/R_y = 0$), Cylindrical ($a/R_x = 0, b/R_y = 0.2$) & Spherical ($a/R_x = b/R_y = 0.2$) has investigated.

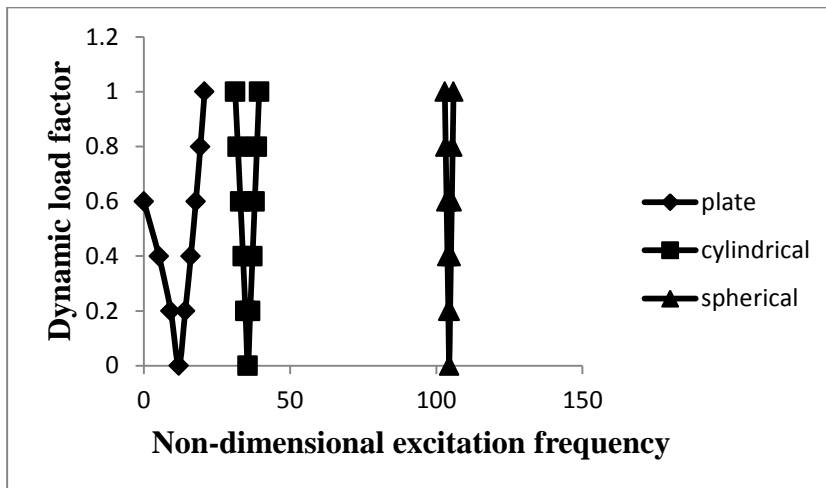


Fig33: Variations of curvature of composite laminated symmetric cross-ply (0/90/90/0) curved panel with elevated temperature

It is observed that the excitation frequency increases with introduction of curvatures from plate to doubly curved panel in elevated temperature. The onset of dynamic instability region occurs earlier with wider dynamic instability region (DIR) coming from spherical laminated composite shell panel to laminated composite flat panel subjected to uniform distribution of temperature.

4.6.5 Effects of Aspect Ratio on excitation frequency

The variation of instability region with dynamic load factor of composite laminated simply supported symmetric cross-ply and anti-symmetric angle-ply shells with excitation frequency subjected to uniform distribution of elevated temperature with different aspect ratio ($a/b = 1, 2$ & 3) are shown in figures 34 & 35. From the fig. it is observed that the onset of instability occurs earlier with decrease of the aspect ratio with decreasing width of instability region & the onset of instability occurs latter for rectangular anti-symmetric angle-ply laminated composite shells than square shells subjected to elevated temperature but with wider instability regions. The width of instability regions increased marginally for rectangular plates than square plates with uniform rise in temperature and moisture concentration. The increase in aspect ratio shifts the frequency of instability region to higher values and reduces the dynamic stability strength. As a result the plates having higher values of aspect ratios are dynamically unstable in elevated temperature and lose its stiffness.

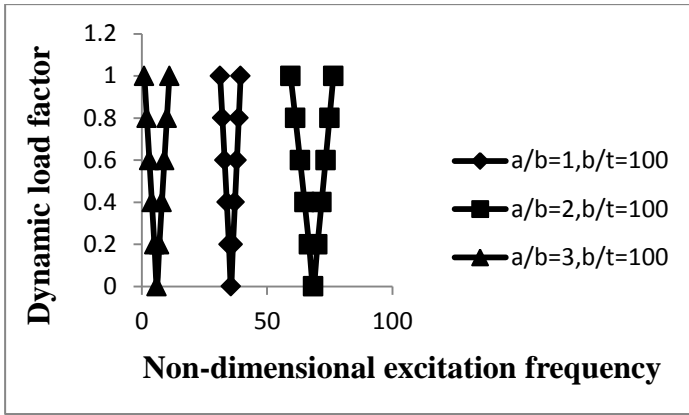


Fig.34: Effect of aspect ratio on instability region of (0/90/90/0) laminate for elevated temperature

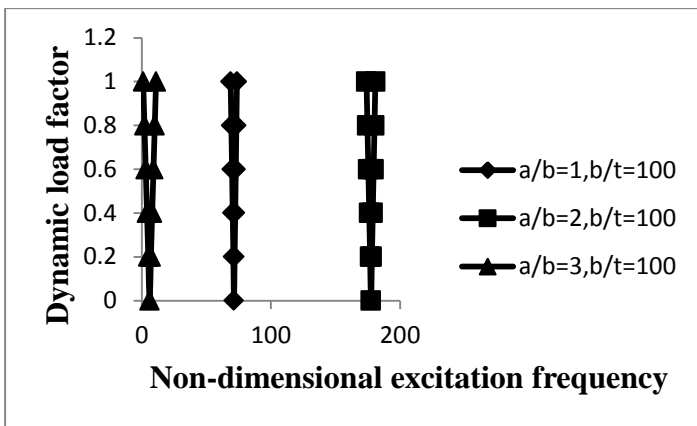


Fig.35: Effect of aspect ratio on instability region of (45/-45/45/-45) laminate for elevated temperature

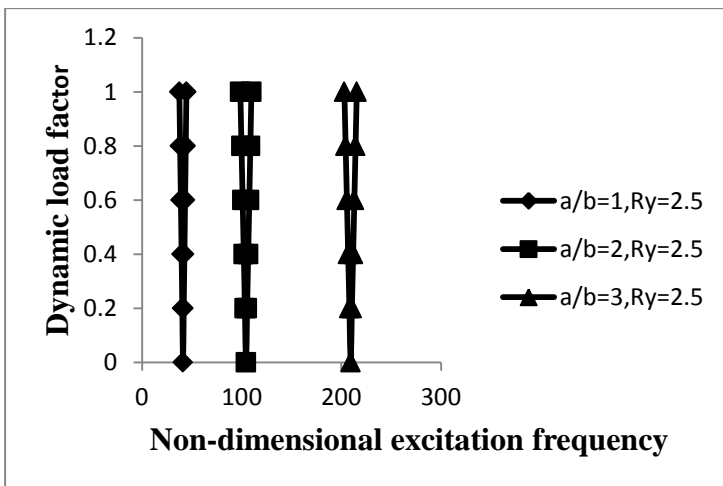


Fig.36: Effect of aspect ratio on instability region of (0/90/90/0) laminate for elevated moisture

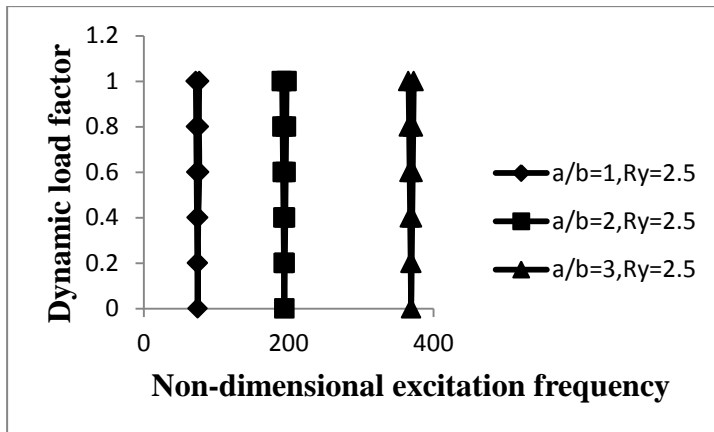


Fig.37: Effect of aspect ratio on instability region of (45/-45/45/-45) laminate for elevated moisture

The variation of instability region with dynamic load factor of composite laminated simply supported symmetric cross-ply and anti-symmetric angle-ply shells with excitation frequency subjected to uniform distribution of elevated moisture with different aspect ratio ($a/b = 1, 2$ & 3) are shown in figures 36 & 37. From the fig. it is observed that the onset of instability occurs earlier with decrease of the aspect ratio with decreasing width of instability region & the onset of instability occurs latter for rectangular anti-symmetric angle-ply laminated composite shells than square shells subjected to elevated moisture but with wider instability regions. The width of instability regions increased marginally for rectangular shells than square shells with uniform rise in moisture concentration. The increase in aspect ratio shifts the frequency of instability region to higher values and reduces the dynamic stability strength. As a result the shells having higher values of aspect ratios are dynamically unstable in elevated moisture condition and lose its stiffness.

4.6.6 Effects on Degree of orthotropy

The variation of excitation frequency with dynamic load factor of composite laminated simply supported symmetric cross-ply and for anti-symmetric angle-ply shells subjected to uniform distribution of temperature are shown in figures 38 & 39. The effect of degree of orthotropy is studied for $E_1/E_2 = 40, 20, 10$ keeping other material properties constant.

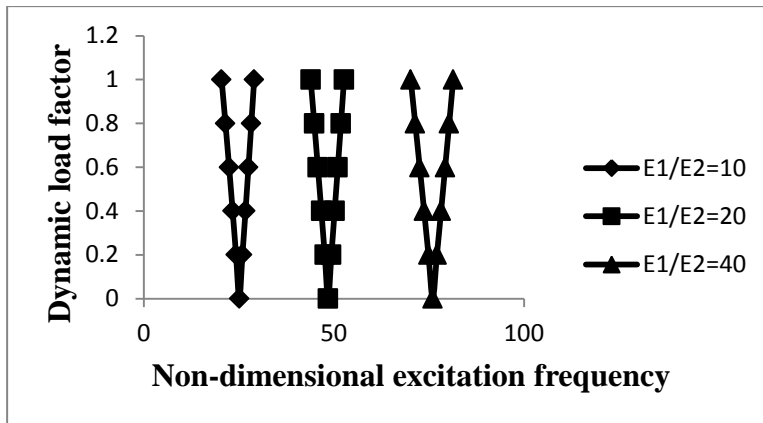


Fig.38: Effect of degree of orthotropy on instability region of (0/90/90/0) laminate for elevated temperature

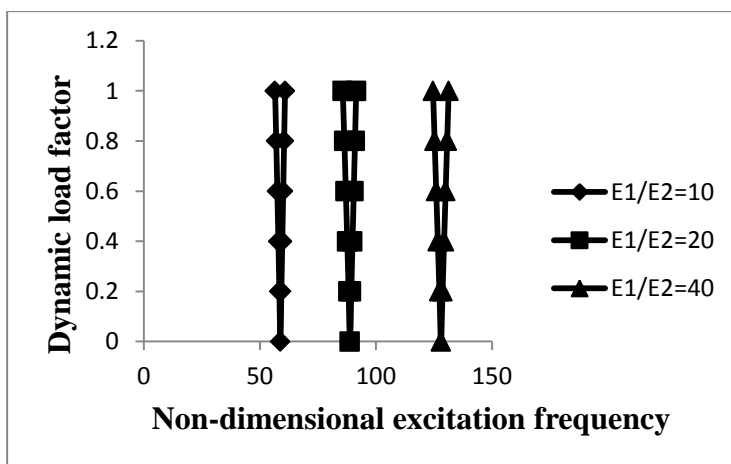


Fig.39: Effect of degree of orthotropy on instability region of (45/-45/45/-45) laminate for elevated temperature

It is observed that the onset of instability occurs latter with increase of degree of orthotropy for symmetric cross-ply and anti-symmetric angle-ply laminated composite shells subjected to elevated temperature but with wider instability regions. The excitation frequency is reduced but the instability region is wider in cross-ply symmetric laminate rather than anti-symmetric angle-ply laminate.

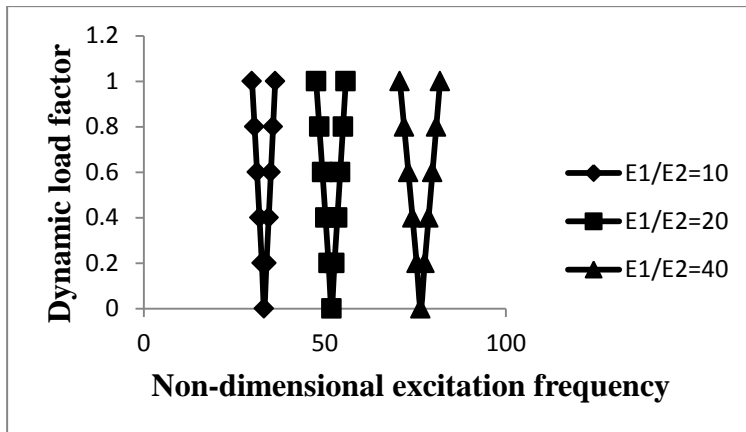


Fig.40: Effect of degree of orthotropy on instability region of (0/90/90/0) laminate for elevated moisture

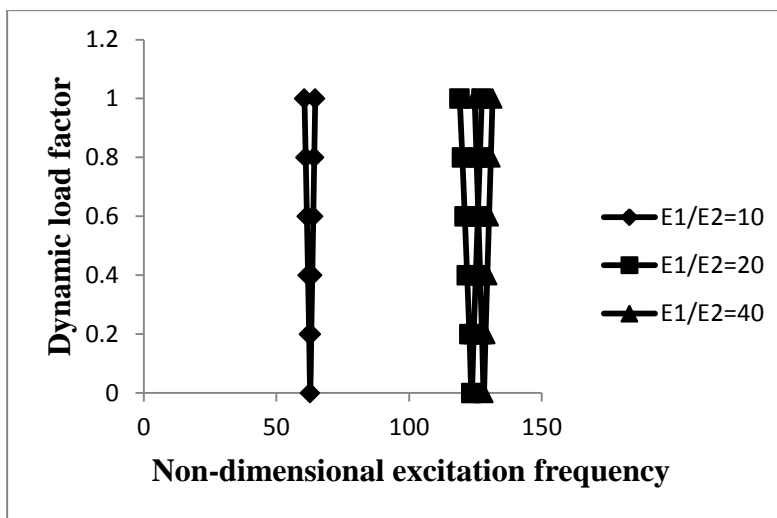


Fig.41: Effect of degree of orthotropy on instability region of (45/-45/45/-45) laminate for elevated moisture

The variation of excitation frequency with dynamic load factor of composite laminated simply supported symmetric cross-ply and for anti-symmetric angle-ply shells subjected to uniform distribution of moisture are shown in figures 40 & 41. The effect of degree of orthotropy is studied for $E_1/E_2 = 40, 20, 10$ keeping other material properties constant. It is observed that the onset of instability occurs latter with increase of degree of orthotropy for symmetric cross-ply and anti-symmetric angle-ply laminated composite shells subjected to uniform distribution of moisture but with wider instability regions. The excitation frequency is reduced but the instability region is wider in cross-ply symmetric laminate rather than anti-symmetric angle-ply laminate.

4.6.7 Effect of Thickness

The variation of excitation frequency with dynamic load factor of composite laminated simply supported symmetric cross-ply and for anti-symmetric angle-ply shells subjected to uniform distribution of temperature are shown in figures 42 & 43. The effect of radius to thickness ratio is studied for $R_x/h = R_y/h = 625, 500, 375$ keeping other geometries and material properties constant. It is observed from the fig. that the onset of dynamic instability region occurs earlier with increase of R_y/h ratio but with wider instability region. The excitation frequency is reduced but the instability region is wider in cross-ply symmetric laminate rather than anti-symmetric angle-ply laminate in elevated temperature.

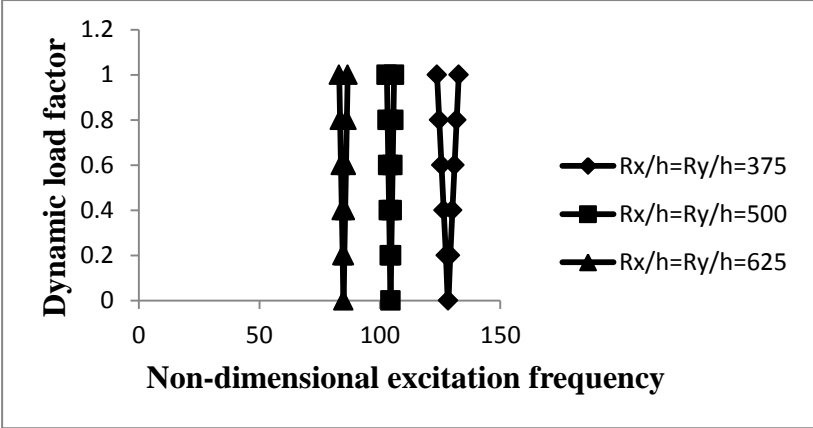


Fig.42: Effect of thickness on instability region of (0/90/90/0) laminate for elevated temperature ($R_x = R_y = 3.125, 2.5, 1.875$)

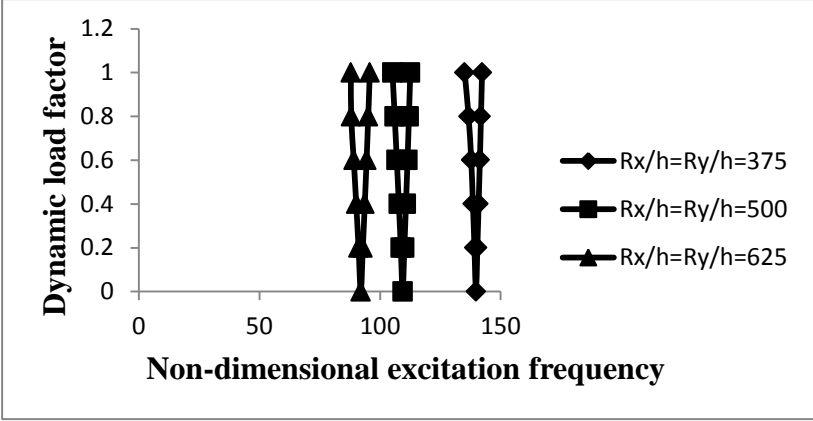


Fig.43: Effect of thickness on instability region of (45/-45/45/-45) laminate for elevated temperature ($R_x = R_y = 3.125, 2.5, 1.875$)

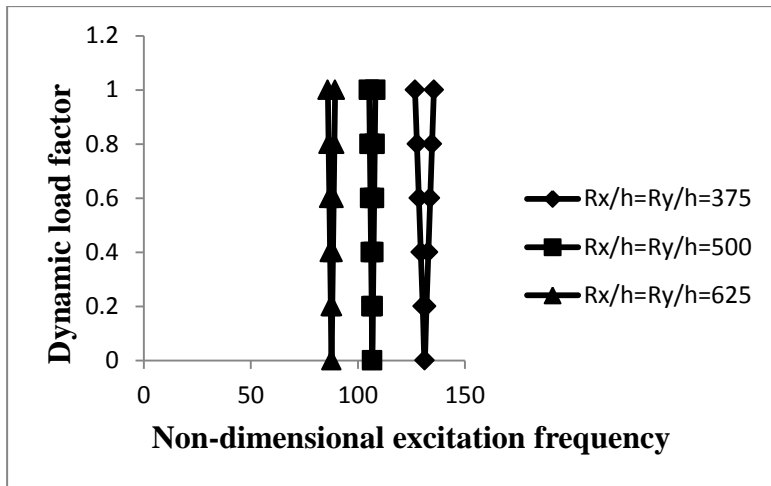


Fig.44: Effect of thickness on instability region of (0/90/90/0) laminate for elevated moisture ($R_x = R_y = 3.125, 2.5, 1.875$)

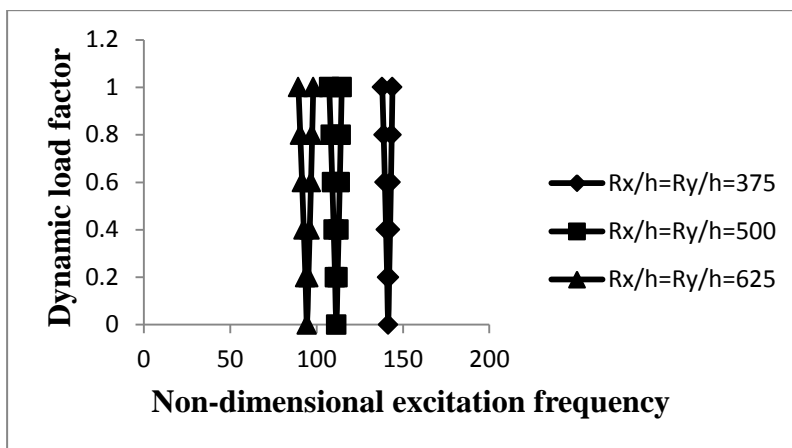


Fig.45: Effect of thickness on instability region of (45/-45/45/-45) laminate for elevated moisture ($R_x = R_y = 3.125, 2.5, 1.875$)

The variation of excitation frequency with dynamic load factor of composite laminated simply supported symmetric cross-ply and for anti-symmetric angle-ply shells subjected to uniform distribution of moisture are shown in figures 44 & 45. It is observed from the fig. that the onset of dynamic instability region occurs earlier with increase of R_y/h ratio but with wider instability region. The excitation frequency is reduced but the instability region is wider in cross-ply symmetric laminate rather than anti-symmetric angle-ply laminate in elevated moisture.

4.6.8 Effect of shallowness ratio

The variation of excitation frequency with dynamic load factor of composite laminated simply supported symmetric cross-ply and for anti-symmetric angle-ply shells subjected to uniform distribution of temperature are shown in figures 46 & 47. The effect of shallowness ratio on instability regions is studied for $R_x/a = R_y/b = 3, 5, 10$ keeping other geometries and material

properties constant. As seen from the fig., the instability excitation frequency is higher for decrease of shallowness by decreasing R_x and R_y . The onset of instability occurs earlier with increase of shallowness ratio but with wide instability region. The excitation frequency is reduced but the instability region is wider in cross-ply symmetric laminate rather than anti-symmetric angle-ply laminate in elevated temperature.

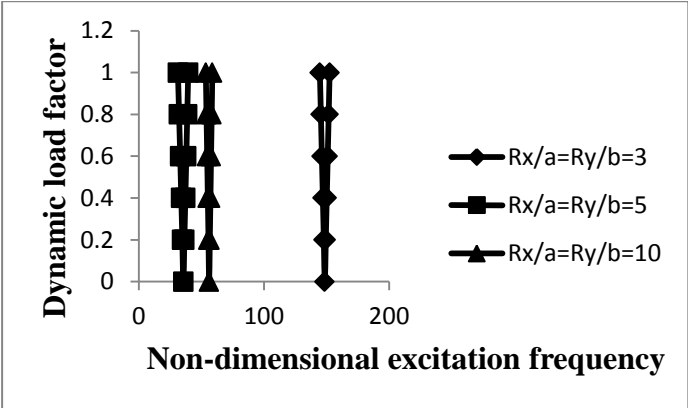


Fig.46: Effect of R_y/b on instability region of (0/90/90/0) laminate for elevated temperature ($R_x = 1.5, 2.5, 5$)

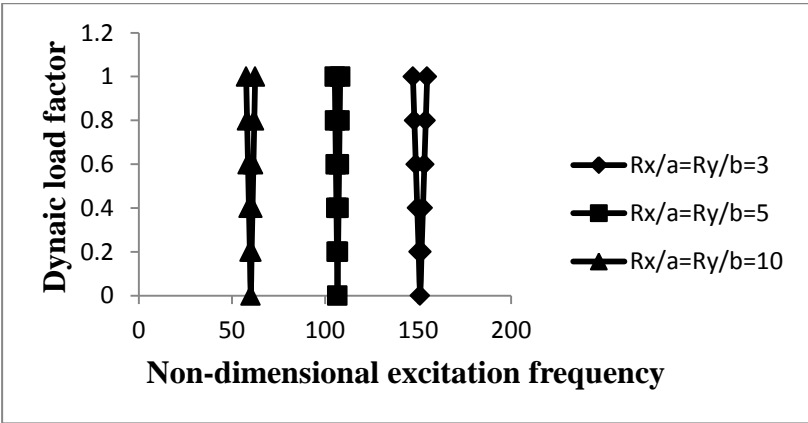


Fig.47: Effect of R_y/b on instability region of (0/90/90/0) laminate for elevated moisture ($R_x = 1.5, 2.5, 5$)

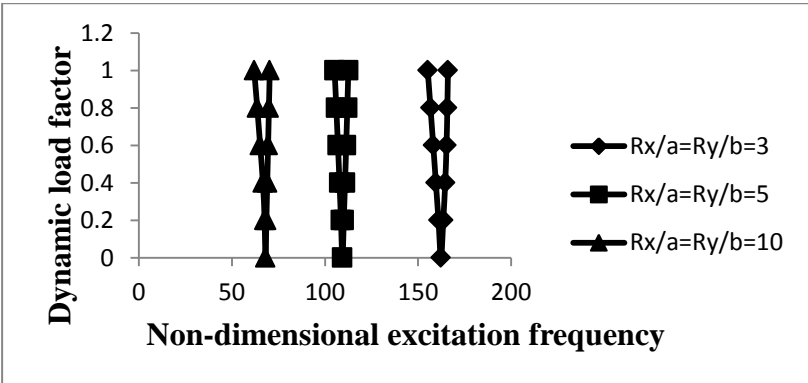


Fig.48: Effect of R_y/b on instability region of (45/-45/45/-45) laminate for elevated temperature ($R_x = 1.5, 2.5, 5$)

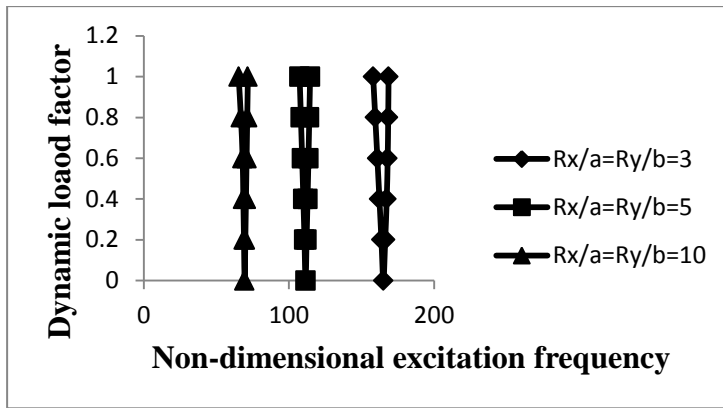


Fig.49: Effect of R_y/b on instability region of (45/-45/45/-45) laminate for elevated moisture ($R_x = 1.5, 2.5, 5$)

The variation of excitation frequency with dynamic load factor of composite laminated simply supported symmetric cross-ply and for anti-symmetric angle-ply shells subjected to uniform distribution of moisture are shown in figures 48 & 49. The effect of shallowness ratio on instability regions is studied for $R_x/a = R_y/b = 3, 5, 10$ keeping other geometries and material properties constant. As seen from the fig., the excitation frequency is higher for decrease of shallowness by decreasing R_x and R_y . The onset of instability occurs earlier with increase of shallowness ratio but with wide instability region. The excitation frequency is reduced but the instability region is wider in cross-ply symmetric laminate rather than anti-symmetric angle-ply laminate in elevated moisture.

4.6.9 Effect of Ply-Orientation

The variation of instability region with dynamic load factor of composite laminated simply supported anti-symmetric angle-ply shells with excitation frequency subjected to uniform distribution of temperature with different ply orientation is shown in fig. 50. It is observed that the onset of instability occurs earlier for anti-symmetric angle-ply laminated composite shells with 0 degree of ply orientation than the shells with higher degree of ply orientation subjected to elevated moisture condition but with narrow DIR. The value of ply orientation for which the instability region is narrower is 45 and for the wider DIR the ply orientation value is 0. The instability region is less wide for increase in lamination angle but the excitation frequencies are decreased with decrease in uniform temperature distribution. The ply orientation for 0^0 seems to be the preferential ply orientation for the lamination sequence which is due to dominance effect of bending-stretching coupling.

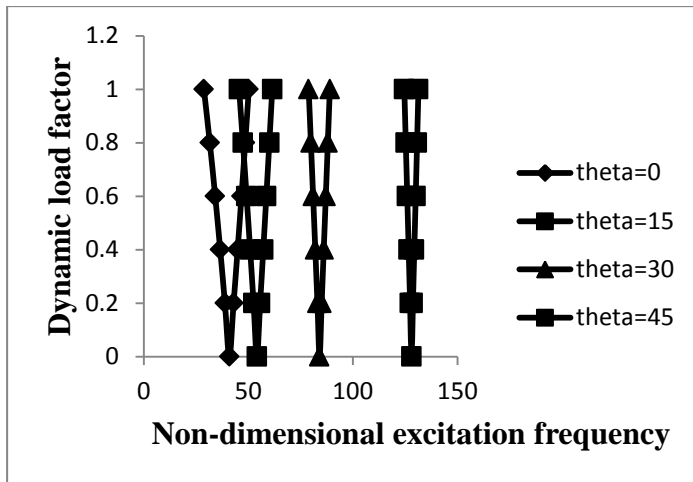


Fig.50: Effect of different ply orientation on instability region of anti-symmetric angle-ply laminate for elevated temperature

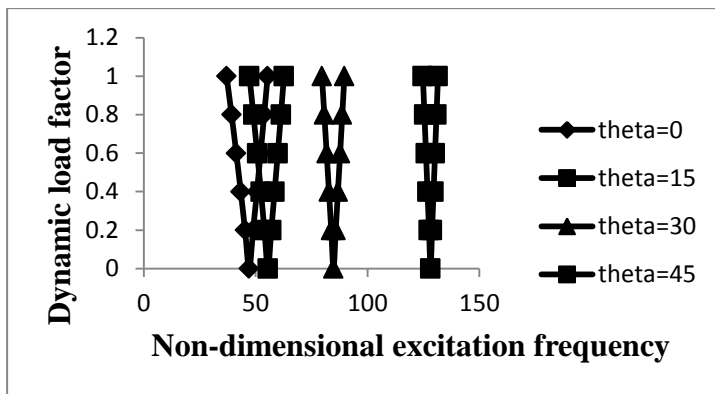


Fig.51: Effect of different ply orientation on instability region of anti-symmetric angle-ply laminate for elevated moisture

The variation of instability region with dynamic load factor of composite laminated simply supported anti-symmetric angle-ply shells with excitation frequency subjected to uniform distribution of moisture with different ply orientation is shown in fig. 51. It is observed that the onset of instability occurs earlier for anti-symmetric angle-ply laminated composite shells with 0 degree of ply orientation than the shells with higher degree of ply orientation subjected to elevated moisture condition but with narrow DIR. The value of ply orientation for which the instability region is narrower is 45 and for the wider DIR the ply orientation value is 0. The instability region is less wide for increase in lamination angle but the excitation frequencies are decreased with decrease in uniform moisture concentration.

CONCLUSIONS

In the present work, the conventional finite element formulation is modified to study the hygrothermal effects on the free vibration and stability of laminated composite shells. The formulation and program developed are general in nature and can handle non-uniform distributions of moisture and temperature. The numerical results are presented and discussed in above. The broad conclusions that can be made from the present study are summarized as follows:

- The fundamental natural frequency decreases with increasing in temperature and moisture concentration.
- The percentage of reduction of fundamental natural frequency with the increase in temperature and moisture concentration is more for both cross-ply and angle-ply symmetric laminates in comparison to anti-symmetric laminates.
- The reduction of fundamental natural frequency with increase in temperature and moisture is more for both symmetric and anti-symmetric cross-ply laminates in comparison to angle-ply laminates.
- The critical load decreases with increasing in temperature and moisture concentration.
- With increase in temperature the reduction in critical loads is non-linear.
- With increase in uniform moisture concentration, the reduction in critical load is nearly linear.
- The excitation frequencies of laminated composite panels decrease with increase of temperature due to reduction of stiffness for all laminates.
- The excitation frequencies of laminated composite panels also decrease substantially with increase of moisture concentration for all laminates.
- Due to static component of load, the onset of instability shifts to lower frequencies with wide instability regions of the laminated composite panels.
- The instability region is observed to be influenced by the lamination angle & increasing the thickness of the plates results in better dynamic stability strength.
- Increasing the aspect ratio, shifts the frequencies of instability region to higher values and reduces the dynamic stability strength.
- The width of dynamic instability region is smaller for square panels than rectangular panels.

- The onset of instability occurs with smaller excitation frequency for thin plates than thick plates. The dynamic instability is less for thick plates than thin plates.

From the present studies, it is concluded that the instability behavior of laminate composite plates and shells is greatly influenced by the geometry, lamination parameter and hygrothermal condition. So the designer has to be cautious while dealing with structures subjected to hygrothermal loading. This can be utilized to the advantage of tailoring during design of laminated composite structures in hygrothermal environment.

Further Scope of Research

The possible extensions to the present study are as presented below:

- The present investigation can be extended to dynamic stability of stiffened plates and shells subjected to hygrothermal condition.
- The present investigation can be extended to dynamic stability of delaminated plates and shells subjected to hygrothermal condition.
- The present study can be extended to dynamic stability of plates and shells involving arbitrary shaped openings subjected to hygrothermal condition.
- The effects of damping on instability regions of plates and shells can be studied.
- The present study deals with structures subjected to conservative forces. This may be extended to non-conservative forces like follower loading.
- The present study can be extended to include the works relating to large deflection and large amplitude vibration analyses of dynamic stability of plates and shells subjected to hygrothermal condition.
- Material nonlinearity may be taken into account in the formulation for further extension of the dynamic stability of plates and shells subjected to hygrothermal condition.
- The plates and shells studied here are of uniform thickness. The elements can be modified to incorporate the geometry of varying thickness.
- Besides all these, there is a large scope experimental investigation on dynamic stability of plates and shells subjected to hygrothermal condition.

BIBLIOGRAPHY

1. **Adams DF, Miller AK.**, “Hygrothermal micro stress in unidirectional composite exhibiting inelastic materials behavior”. *Journal of Composite Material* 1977; 11:285–99.
2. **Argento A., Scott R.A.**, “Dynamic instability of laminated anisotropic circular cylindrical shells”, part II: numerical results, *J.Sound Vib.*162(2) (1992) 323-332.
3. **Argento A.**, Dynamic stability of a composite circular cylindrical shell subjected to combined axial and torsional loading, *J.Compos. Mater.*27 (18)
4. **Babu C. Sarath., and Kant T.**, “Refined higher order finite element models for thermal buckling of laminated composite and sandwich plates”, *J of Therm Stres*, 23 (2000),111130.
5. **Balamurugan, V., Ganapathi, M., and Varadan,T.K.**, “Nonlinear dynamic instability of laminated composite plates using finite element method”. *Computers and Structures*, 60(1), 125-130,1996.
6. **Bert, C.W. and Birman, V.**, “Parametric instability of thick, orthotropic, circular cylindrical shells”. *Acta Mechanica*, 1988,71,61-76.
7. **Bhimaraddi A, Chandrashekhara K.**, “Nonlinear vibrations of heated anti-symmetric angle-ply laminated plates”. *Int J Solids Struct* 1993;30:1255–568.
8. **Birman V.**, Dynamic stability of unsymmetrically laminated rectangular plates, *Mech Res. Commun.* 12 (1985) 81-86.
9. **Birman, V. and Bert, C.W.**, “Dynamic stability of reinforced composite cylindrical shells in thermal fields”. *Journal of Sound and vibration*, 1990, 142, 183-190.
10. **Bodner V. A.**, The stability of plates subjected to longitudinal periodic forces, *Prikl. Mat. Mekh.* (N.S) 2 (1938) 87-10
11. **Bolotin,V.V.**,“The Dynamic stability of elastic systems”. HoldenDay,SanFrancisco,1964
12. **Botelho. E.C., Pardini.L.C., and Rezende M.C.** “Hygrothermal Effect on the damping behaviour of metal/glass fibre/epoxy hybrid composites,” *J of Mate Scie and Engin A*, 399 (2005), 190-198.
13. **Bowles DE, Tompkins SS.** “Prediction of coefficients of thermal expansion for unidirectional composite”. *J Compos Mater* 1989;23:370–87.
14. **Carrera E, Krause H.** “An investigation of nonlinear dynamics of multilayered plates accounting for C^0 requirements”. *Comput Struct* 1998;69:473–86.

15. **Cederbaum G.**, Dynamic stability of shear deformable laminated plates, *AIAA Journal*, 29 (1991), 2000-2005.
16. **Chakrabarti A. and Sheikh A.H.**, Dynamic instability of laminated sandwich plates using an efficient finite element model, *Thin-Walled Struct*, **44** (2006) 57-68.
17. **Chakrabarti A. and Sheikh A.H.**, Dynamic instability of laminated sandwich plates subjected to in-plane partial edge loading, *Ocean Engg*, **33** (2006) 2287-2309.
18. **Chung-Yi Lin and Lien-wen Chen**, Dynamic stability of rotating pre-twisted blades with a constrained damping layer, *Compo Struct*, 61, (2003), 235-245.
19. **Crispino D. J. and Benson R. C.**, Stability of twisted orthotropic plates, *International J. of Mech Scie*, 28 (6) , 371-379.
20. **Dey P., Singha M.K.**, Dynamic stability analysis of composite skew plates subjected to periodic in-plane load, *Thin-Walled Struct*, **44** (2006) 937-942.
21. **Duffield R. C. and Williams N.**, Parametric Resonance of stiffened rectangular plates, *J. appl.Mech. Trans. ASME Ser. E*, 40 (1973) 217-226.
22. **Eslami, M.R., Shariyat, M., 1999.** A higher-order theory for dynamic buckling and postbuckling analysis of laminated cylindrical shells, *Journal of Pressure Vessel Technology ASME* 121, 94-102.
23. **Eslami, M.R., Shariyat, M., Shakeri, M., 1998.** Layerwise theory for dynamic buckling and postbuckling of laminated composite cylindrical shells. *AIAA Journal* 36, 1874-1882.
24. **Flaggs, D.L., Vinson, J.R., 1978.** Hygrothermal effects on the buckling of laminated composite plates. *Fibre Science and Technology* 11, 353-365.
25. **Ganapati, M., Patel, B.P., Boisse, P., and Touratier, M.** "Nonlinear dynamic stability characteristics of elastic plates subjected to periodic in-plane load". *International journal Non-linear Mechanics*, 35,467-480, 2000.
26. **Ganapathi M., Patel B.P., Pawargi D.S.,**"Dynamic analysis of laminated cross-ply composite non-circular thick cylindrical shells using higher-order theory". *International Journal of Solids and Structures* 39(2002) 5945-5962
27. **Gandhi MV, Usman M, Chao L.** Nonlinear vibration of laminated composite plates in hygrothermal environments. *J Eng Mater Technol* 1998;10:110-4.
28. **Huang, Xiao-Lin, Shen, Hui-Shen and Zheng, Jain-Jun.** "Nonlinear vibration and dynamic response of simply supported shear deformable laminated plates in hygrothermal environments" *Composites Science and Technology* 64, 1419-1435, 2004.

29. **Huang NN, Tauchert TR.** “Large deformations of laminated cylindrical and doubly curved panels under thermal loading”. *Comput Struct* 1991;41(2):303-12.
30. **Ishikawa T, Koyama K, Kobayayaski S,** “Thermal expansion coefficients of unidirectional composites”. *Composite Material* 1978; 12:53–168.
31. **J.C. Yao,** “Nonlinear elastic buckling and parametric excitation of a cylinder under axial loads”, *TASME, J. Appl. Mech.* 29 (1965) 109–115.
32. **Kar R. C. and Ray K.,** “Dynamic stability of a pre-twisted, three layered symmetric sandwich beam,” *J of Sound and Vibr,* 183(4) (1995), 591-606.
33. **Krajanovic D. and Herman G.,** “Numerical solution of the dynamic stability problem”. *Int. J. numer. Meths Engg,* 2 (1970) 551-561.
34. **Kumar L.R, Datta P. K and Prabhakara D. L.,** “Dynamic instability characteristics of laminated composite plates subjected to partial follower edge load with damping”, *Int. J. Mech Sci,* 45(2003) 1429-1448.
35. **Kundu Chinmay Kumar & Han Jae-Hung,** ”Vibration characteristics and snapping behavior of Hygro-thermo-elastic composite doubly curved shells”. *Composite Structures* 91 (2009)306-317
36. **Kundu Chinmay Kumar, Han Jae-Hung,** ”Nonlinear buckling analysis of hygrothermoelastic composite shell panels using finite element method”. *Composites: part B40* (2009) 313-328.
37. **K.M Liew, Y.G.Hu, X. Zhao, T.Y.Ng,** “Dynamic stability analysis of Composite laminated Cylindrical Shells via the mesh-free kp-Ritz method”. *Journal of computer methods in applied mechanics and engg.* **196** ,147-160, 2006
38. **K. Nagai, N. Yamaki,** “Dynamic stability of circular cylindrical shells under periodic compressive forces”, *J. Sound Vibr.* 58 (3) (1978) 425–441.
39. **Lal Achhe, Singh B.N., Kale Sushil,** “Stochastic post buckling analysis of laminated composite cylindrical shell panel subjected to hygrothermomechanical loading”. *Composite Structures* 93 (2011) 1187-1200
40. **Lee SY, Chou CJ, Jang JL, Lim JS.,** ”Hygrothermal effects on the linear and nonlinear analysis of symmetric angle-ply laminated plates”. *Journal of Composite Structure* 1992;21-1:41–8.
41. **Lee SY, Yen WJ.** “Hygrothermal effects on the stability of cylindrical composite shell pane”1. *Comput Struct* 1989;33(2):551-9.
42. **Liao C.L., Cheng C.R.,** “Dynamic stability of stiffened laminated composite plates and sheels subjected to in-plane pulsating forces”, *J. Sound Vib.* 174 (3) (1994) 335-351.

43. **Librescu L, Lin W.** “Vibration of geometrically imperfect panels subjected to thermal and mechanical loads”. *J Spacecraft Rockets* 1996;33(2):285-91.
44. **Librescu L, Lin W, Nemeth MP, Starnes JH.** “Thermomechanical postbuckling of geometrically imperfect flat and curved panels taking into account tangential edge constraints”. *J Thermal Stresses* 1995;18:465–82.
45. **Librescu L, Souza MA.** “Postbuckling of geometrically imperfect shear-deformable flat panels under combined thermal and compressive edge loadings”. *J Appl Mech ASME* 1993;60:526–33.
46. **Marques SPC, Creus GJ.** Geometrically nonlinear finite element analysis of viscoelastic composite materials under mechanical and hygrothermal loads. *Comput Struct* 1994;53(2):449-56.
47. **Nagai K., Yamaki N.,** Dynamic stability of circular cylindrical shells, *Acta Mech.* 71 (1988) 61-76.
48. **Naidu N.V. Swamy, Sinha P.K.,** “Nonlinear free vibration of laminated Composite Shells in Hygrothermal condition”, *Journal of Composite Structures*, **77**, 475-483, 2006.
49. **Naik N.K., Chandra sekhar Y. and Meduri S.,** “Damage in woven-fabric composites subjected to low-velocity impact,” *J of com scie and techn*, 60 (2000), 731-744.
50. **Nath Y, Shukla KK.** “Nonlinear transient analysis of moderately thick laminated composite plates”. *J Sound Vib* 2001;247:507–26
51. **NG T.Y., LAM K.Y. and REDDY J.N.,** “Dynamic stability of cross-ply laminated composite cylindrical shells” *Int, J.Mech.sci.*vol.40.No.8.pp.805-823, 1998
52. **Nosier, A. and Reddy, J. N.,** “Vibration and stability analysis of cross-ply laminated circular cylindrical shells”. *Journal of Sound and Vibration*, 1992, 157, 139-159.
53. **Panda S.K. & Singh B.N.,**”“Large amplitude free vibration analysis of thermally post-buckled composite doubly curved panel using non-linear FEM”. *Finite Elements in Analysis and Design* 47(2011) 378-386
54. **Parhi P.K., Bhattacharyya S.K., Sinha PK,**” Hygrothermal effects on the dynamic behavior of multiple delaminated composite plates and shells” *J Sound Vib* 2001;248(2):195-214
55. **Patel BP, Ganapathi M, Makhecha DP.** Hygrothermal effects on the structural behavior of thick composite laminates using higher order theory. *Journal of Composite Structure* 2002;56:25–34.
56. **Pearson CE.** “Numerical methods in engineering and science”. NewYork: Van Nostrand Reinhold; 1996.

57. **Qatu MS, Leissa AW.**, “Buckling or transverse deformations of unsymmetrically laminated plates subjected to in-plane loads”. *AIAA Journal* 1993;31:189-194.
58. **Ram KSS, Sinha PK.**, “Hygrothermal effects on the buckling of laminated composite plates”. *Journal of Composite Structures* 1992;21:233-47.
59. **Ram KSS, Sinha PK.** “Vibration and buckling of laminated plates with a cutout in hygrothermal environment”. *AIAA J* 1992;30:2353-5.
60. **Rao VVS, Sinha PK.**, “Bending characteristic of thick multidirectional composite plates under hygrothermal environment”. *Reinforced Plastics Composite* 2004;23:1481-95.
61. **Reddy J.N.** “Exact solutions of moderately thick laminated shells”. *Journal of Engineering Mechanics, ASCE*, 110(5), 794-809, 1984.
62. **Reddy JN.** “Geometrically nonlinear transient analysis of laminated composite plates”. *AIAA J* 1983;21:621-9
63. **Reddy, J.N., Liu, C.F., 1985.** “A higher-order shear deformation theory of laminated elastic shells”. *International Journal of Engineering Sciences* 23, 319-330.
64. **Reddy, J.N., Savoia, M., 1992.** Layer-wise shell theory for post buckling of laminated circular cylindrical shells. *AIAA Journal* 30, 2148-2154.
65. **Ribeiro P., Jansen E.,** “Non-linear vibrations of laminated cylindrical shallow shells under thermomechanical loading” . *Journal of Sound and Vibration* 315(2008)626-640
66. **Sai Ram KS, Sinha PK.**, “Hygrothermal effects on the bending characteristics on laminated composite plates”. *Journal of Composite Structures* 1991;40:1009-15.
67. **Sahu S. K. and Asha A. V.,** Parametric resonance characteristics of angle-ply twisted curved panels, *Int. J. of Struct Stab and Dynam*, 8 (1) (2008) 61-76.
68. **Sahu S.K. and Dutta P.K.** “Dynamic stability behavior of laminated composite curved panel with cutout”. *Journal of Engineering Mechanics, (ASCE)*0733-9399,129:11, 1245(2003)
69. **Sahu S. K. and Datta P. K.,** Dynamic instability of laminated composite rectangular plates subjected to non-uniform harmonic in-plane edge loading, *Journal of Aerospace Engg. Proc. Of Inst of Mech Eng, Part G*, 214 (2000), 295-312.
70. **Sahu S. K. and Datta P. K.,** Parametric instability of laminated composite curved panels, *IE (I) J-AS*, (2000) 20-24.
71. **Sahu S. K. and Datta P. K.,** Parametric resonance characteristics of laminated composite doubly curved shells subjected to non-uniform loading, *J of Reinf Plast and Compos*, 20(18) (2001), 1156- 1576.

72. **Sen Y. Lee, Wen J.Yen,** "Hygrothermal effects on the stability of a cylindrical composite shell panel" *Computers & Structures* volume 33, Issue 2, 1989,Pages 551-559
73. **Shen HUI-Shen** "Hygrothermal effects on the post buckling of composite laminated cylindrical shells". *Journal of composite science & technology* 60 (2000)1227-1240
74. **Shen Hui-Shen,** "The effects of hygrothermal conditions on the postbuckling of shear deformable laminated cylindrical shells", *International Journal of Solids and Structures* 38(2001)6357-6380
75. **Shen HS.,** "Hygrothermal effects on the nonlinear bending of shear deformable laminated plates". *Journal of Engineering Mechanics* 2002;128:493–6.
76. **Shen H-S,** Hygrothermal effects on the post buckling of shear deformable laminated plates. *Int J Mech Sci* 2001;43:1259-81
77. **Shen H-S,** The effects of hygrothermal conditions on the postbuckling of shear deformable laminated cylindrical shells. *Int J Solids Struct* 2001;38:6357-80.
78. **Shen H-S,** Hygrothermal effects on the post buckling of axially loaded shear deformable laminated plates cylindrical panels *Compos Struct* 2002;56:73-85.
79. **Singh B.N. and Verma V.K.** "Hygrothermal effects on the buckling of laminated composite laminated plates with random geometric and material properties", *J of Reinf Plast and Comps*, 28(2008), 409-427.
80. **Singh G, Rao GV, Iyengar NGR.** "Finite element analysis of the nonlinear vibrations of moderately thick unsymmetrically laminated composite plates". *J Sound Vib* 1995;181:315–29.
81. **Snead JM, Palazotto AN.,** "Moisture and temperature effects on the instability of cylindrical composite panels". *Journal of Aircraft* 1983;20:777}83.
82. **Srinivasan R.S. and Chellapandi. P.** Dynamic stability of rectangular laminated composite plates, *Compu and Struc*, 24 (2) (1986) 233-238.
83. **Strife JR, Prewo KM.,** "The thermal expansion behavior of unidirectional and bidirectional Kevlar/epoxy composites". *Journal of Composite Material* 1979;13:264–7.
84. **Timoshenko, S. P. and Gere, J. M.,** "Theory of Elastic Stability". McGraw-Hill, New York, 1961.
85. **Thangaratnam K.R., Palaninathan. and Ramachanran J..** "Thermal buckling of composite laminated plates", *Compu and Struc*, 32(1989),1117-1124.
86. **Tsai SW, Hahn HT.,** "Introduction to composite materials". Westport, CT: *Technomic Publishing Co*, 1980.

87. **Udar R.S., Datta P. K.**, Dynamic analysis of parametrically excited laminated composite panels under non-uniform edge loading with damping, *Compu and Struc*, 79 (2007) 356-368.
88. **Vijayaraghavan A., Evan-Iwanowski R.M.**, Parametric instability of circular cylindrical shells, *TASME, J. Appl. Mech.* 31 (1967) 985-990.
89. **V.V. Bolotin**, “The Dynamic Stability of Elastic Systems”, Holden-Day, San Francisco, 1964.
90. **Whitney JM, Ashton JE.**, “Effect of environment on the elastic response of layered composite plates”. *AIAA* 1971;9: 1708–13.
91. **Yao J.C.**, Nonlinear elastic buckling and parametric excitation of a cylinder under axial loads, *TASME.J. Appl. Mech* 29 (1965) 109-115.